5 Results and Discussion

5.1 Preformulation Studies

5.1.2 Sample drugs identification

The drug samples were identified using various parameters and were confirmed for their identity based on Organoleptic properties, melting point determination, infrared spectroscopy, ultraviolet spectroscopy. The sample drugs, Rifabutin was an odorless, white to off-white crystalline substance was per reported values (LeBel, et al.,1998).

5.1.3 Melting point determination

The drug was further conformed by melting point as the sample drugs showed a characteristic melting point when melted in the reported range. The melting point of Rifabutin was found to be 165-176°C which was nearer to the reported value of standard drug (171.2^{o}C) (Nighute, et al.,2009).

5.1.4 Solubility of Sample drugs

Solubility of Rifabutin in different solvent systems has been reported in Table 5.1 RIF hardly dissolves in aqueous media and practically insoluble in water at acidic and neutral pH, and soluble in organic solvent media (Muttil, et al.,2007).

Table: 5. 1 -Solubility profile of Rifabutin in different solvent

Sl. No.	Solvent	Solubility at 37°C
1.	Distilled water	0.19±0.06 µg/ml
2.	Phosphate buffer pH 7.4	1.7±1.6 mg/ml
3.	Phosphate buffer pH 4.5	0.79±0.34 µg/ml
6	Methanol	345±0.12 mg/ml
7.	Chloroform	44± 0.34 mg/ml
8.	Ethanol	98±18 mg/ml

Values are mean ±SD; n=3

The solubility of Rifabutin in distilled water, soluble in phosphate buffer (pH 7.4) was found to be 0.19±0.06 mg/ml and 1.7±1.6 mg/ml respectively whereas the solubility of Rifabutin in Phosphate Buffer (pH 4.5) was found to be 0.79±0.34 µg/ml and solubility in Methanol,

Chloroform and Ethanol respectively 345±0.12 mg/ml, 44±0.34 mg/ml, 98±18 mg/ml respectively indicating that the sample drugs has limited solubility in distilled water but were soluble as the pH of the solvents was increased (Benet, et al., 2011).

5.1.5 Partition Coefficient determination

The partition coefficient of the sample of Rifabutin was determined by using n-octanol/distilled water and n-octanol/PBS (pH 7.4) was found to be 6.9±0.17 and 0.82±0.23 respectively suggesting lipophilic nature of the drugs selected (Vostrikov, et al., 2008).

5.2 Analytical method development:

5.2.1 Selecting λ_{max} for Rifabutin

Based on below pictured wavelength scan the λ max was chosen to be 242nm and 278nm. As compared to 278 nm, 242nm was selected and all ensuing measurements were done thus.

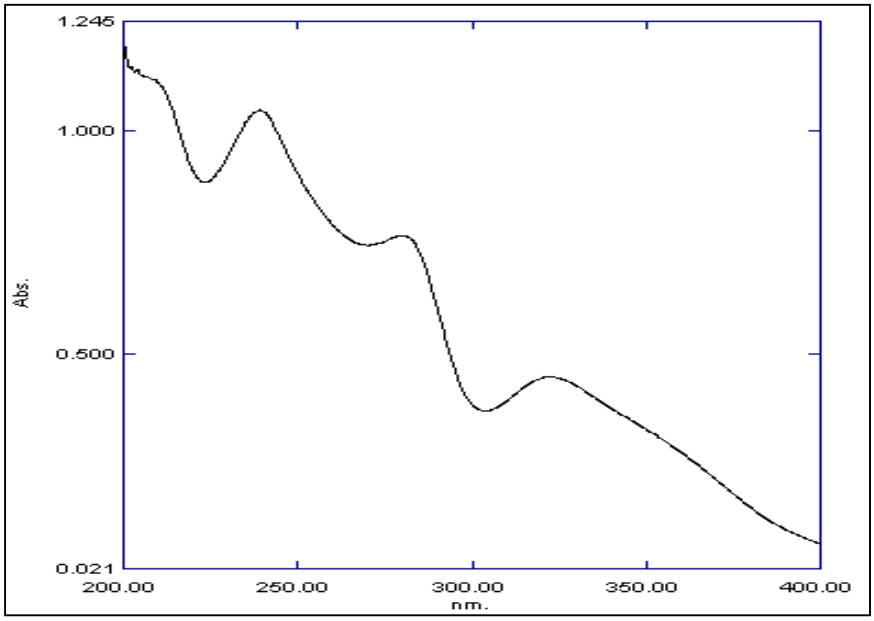

Fig: 5.2- λ_{max} of Rifabutin

5.2.2. Calibration curve of Rifabutin in Water

Six serial dilutions were prepared in a concentration range from 10 to 100 µg/ ml. A volume of 20 µl from each concentration of the solution was injected, and chromatograms were recorded three independent determinations were performed at each concentration. A linear calibration graph (y=0.01x+1; where y and x are peak area and concentration, respectively) was obtained over six concentrations 10, 20, 40, 60, 80, 100 µg/ml. A correlation coefficient was found to be 0.9802 (Polk, et al., 2001) (Trivedi, et al., 2017).

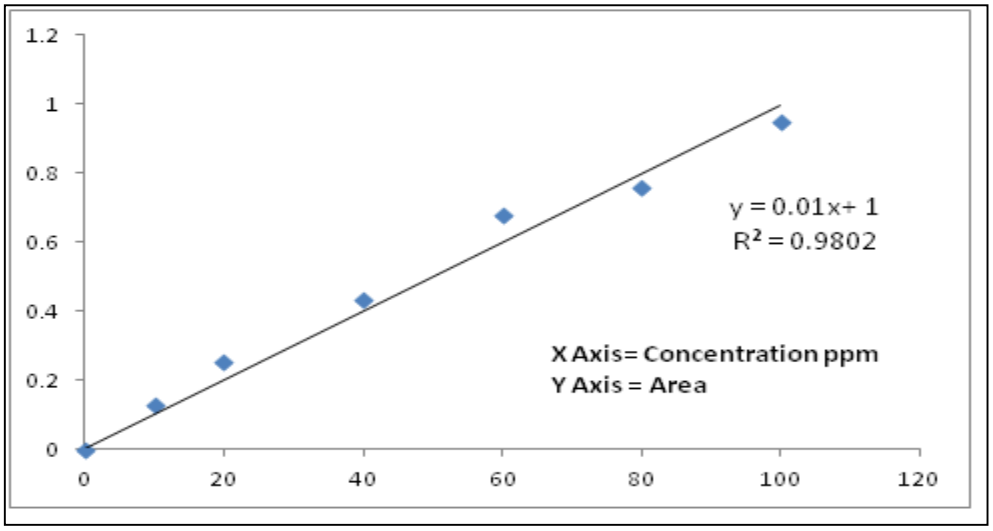

Fig.5.3- Linearity Curve of Rifabutin

5.2.3 Method Development

The method utilizing Acetonitrile + Methanol: Water as mobile phase yielded broad peak, whereas with Acetonitrile + Methanol: Water tailing was observed with acetonitrile and methanol as diluent. During method development, a number of variations were tested like Acetonitrile + Methanol concentration and flow rate to give a symmetric peak. With a mobile phase Acetonitrile + Methanol: Water (75:25) at flow rate 1 ml min-1 and wavelength is 242 nm, the symmetric peak was obtained (Blanchet, et al., 2009) (Sharma, et al., 2012).

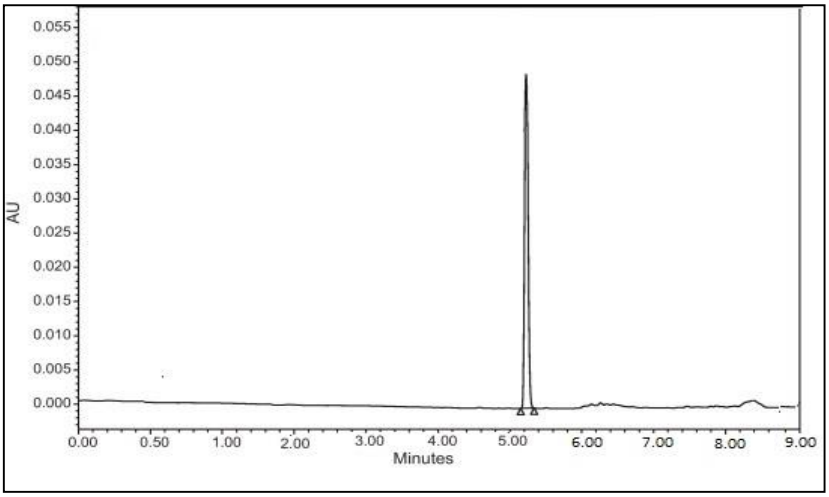

Fig:5.4-Chromatogram of Rifabutin

5.2.4 Validation

5.2.4.1 Accuracy

To ensure the accuracy of the analytical method, the recovery studies were carried out. The known amount of rifabutin was added to a pre-quantified sample solution of its dosage form,

and the amounts of rifabutin were estimated by measuring the peak area ratios and by fitting these values to the straight line equation of calibration curve. The recovery studies were carried out three times over the specified concentration range of rifabutin. The Accuracy was calculated at three different concentrations of drug which is equivalent to 80, 100 and 120% of the active ingredient by calculating the recovery of rifabutin with % RSD (Else, et al., 2010) (Savale, et al.,2017).

Table: 5.2- Recovery Study of Rifabutin

S No.	Concentration Percentage (%)	Concentration of STD (µg ml^{-1})	Concentration of Sample (µg ml^{-1})	Percentage (%) recovery found	Percentage (%) RSD
1	80	100	80	99.71	0.16
2	100	100	100	99.63	0.38
3	120	100	120	99.48	0.47

5.2.4.2 Precision

The intra-day precision of the method was determined by repeat analysis (three identical injections) at three concentration levels. Inter-day precision was established by performing the analysis next day on a freshly prepared solution. The low RSD values of indicate the ruggedness of the method. The low RSD values indicate the ruggedness of the method (Savale, et al.,2017).

Table:5.3-Precision Study of Rifabutin

S No.	Concentration	mean peak area	(±) Standard Deviation	Percentage (%) RSD
Inter Day				
1	20 µg ml^{-1}	1452572.81	2801.58	0.218
2	40 µg ml^{-1}	2688315.80	18723.31	0.639
3	60 µg ml^{-1}	3733491.49	29835.63	0.739
Intra Day				
1	20 µg ml^{-1}	1451482.59	13603.45	0.979
2	40 µg ml^{-1}	2615819.89	20361.59	0.861
3	60 µg ml^{-1}	3436306.11	29302.51	0.839

5.2.4.3 Repeatability

The peak area of 40 ppm drug solution was analysed six times on the same day. The % RSD was calculated for the resultant peak area (Kumar, et al., 2011).

Table:5.4-Repeatability Study

S No	Concentration	Percentage (%) RSD
1	40 µg ml^{-1}	0.62

5.2.4.4 Robustness:

The robustness was assessed by altering the following experimental conditions such as, by changing the flow rate from 0.5 to 1.5 ml/min, the mobile phase composition with Acetonitrile+ Methanol: Water (76:24, 74:26) and analysed in triplicate. In all Chromatographic varied conditions, there was no significant change in chromatographic parameters. There was no effect of mobile phase composition on retention time as seen (Verweij-van Wissen, et al., 2005) (Parikh, et al.,2011).

Table:5.5-Robustness Study (n=3)

Concentration	Conditions changed	Percentage (%) RSD	Mean RT
100 µg ml^{-1}	Mobile Phase Composition		
	76:24	0.51	5.3
	74:26	0.35	5.1
	Flow Rate		
	0.5 ml min^{-1}	1.32	5.2
	1.5 ml min^{-1}	1.47	5.4

5.2.5 Infrared Spectral Assessment

Infrared spectrum of any compound gives information about the groups present in that particular compound. IR spectrum of Rifabutin was taken out using KBr pellets. Various peaks in IR spectra were interpreted for different groups and were matched with reference IR spectra (IP 1996). Sample was Authentic.

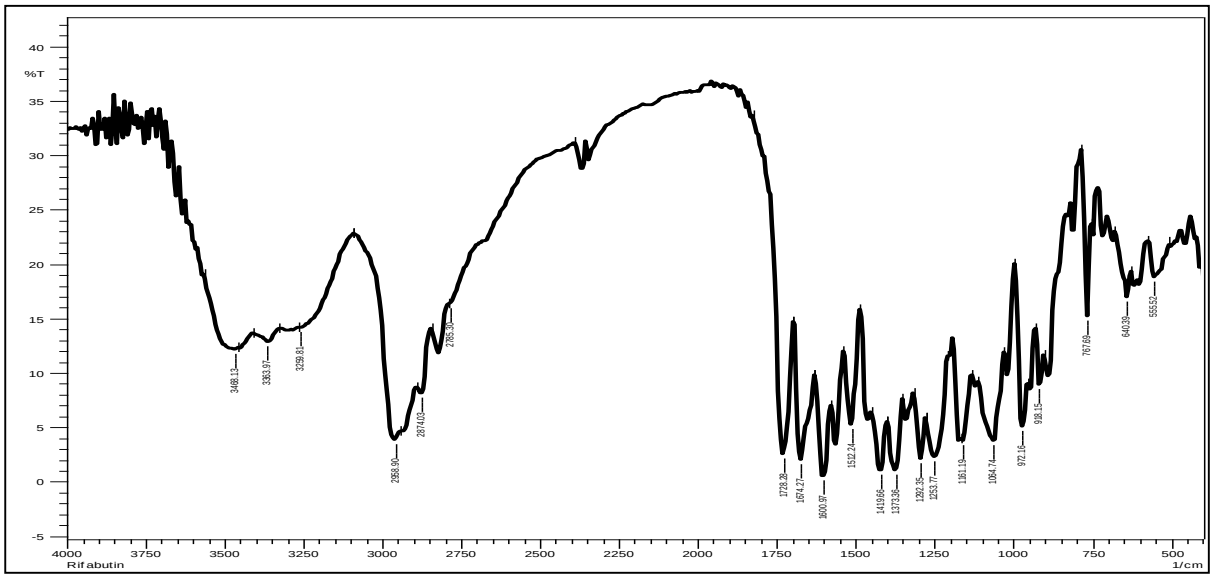

Fig: 5.5- Fourier Transform Infrared (FTIR) of Rifabutin

Table:5.6- Identified Compounds of Rifabutin

S. No	Peak (cm^{-1})	Identified compound
1	1674 and 1600	-C=C- bonds
2	1419 and 1373	C-H and deformation frequency of $–CH_2$
3	1728	C=O stretching vibration
4	2958 and 2947	Presence of symmetric and asymmetric -C-H stretching vibration
5	1373 and 1562	Gemdimethyl groups and –N-H deformation of secondary amino
6	1253 and 1292	Phenolic C-O stretching

The principle absorption peaks observed at 1674 and 1600 of drug RFB could be attributed to the stretching vibrations of aryl ketones and -C=C- bonds. Two peaks at 1419 cm-1 and 1373 cm-1 are possibly from C-H deformation frequency of -CH2 group. An absorption band at 1728 cm-1 of RFB is developed for C=O stretching vibration. Two absorption bands centred at 2958 cm-1 and 2947 cm-1 indicates the presence of symmetric and asymmetric –C-H stretching vibration of aromatic nuclei. The strong IR peaks at 1373 cm-1 and 1562 cm-1 is due to the presence of gemdimethyl groups and –N-H deformation of secondary amino groups respectively. Phenolic C-O stretching vibrations of RFB group are appeared at 1253 and 1292 cm-1. Above identified peaks in IR spectra were presents authentication of Rifabutin sample (Nimje, et al., 2009).

5.3 Solubility of Rifabutin in Different Liquid Lipid

NLCs comprise of both solid and additionally liquid lipids. Liquid lipids or oil for the preparation of NLCs can be chosen in view of the relative solubility of drug. The technique adopted for the determination of solubility of drug in oil was like the strategies utilized as a part of nanoemulsions or self-emulsifying preparation system. The fixed volume (1 mL) of various oils was taken up against 2 ml glass vials independently. An abundance amount of drug was added to every vial and kept in shaker incubator for 72 hr at 37◦C and 150 RPM. The vials containing oil and drug were centrifuged at 5000 RPM for 30 min to isolate the undissolved drug and solubility of the drug was determined in oils by using UV spectroscopicaly at 242 nm (Thorat, et al., 2011).

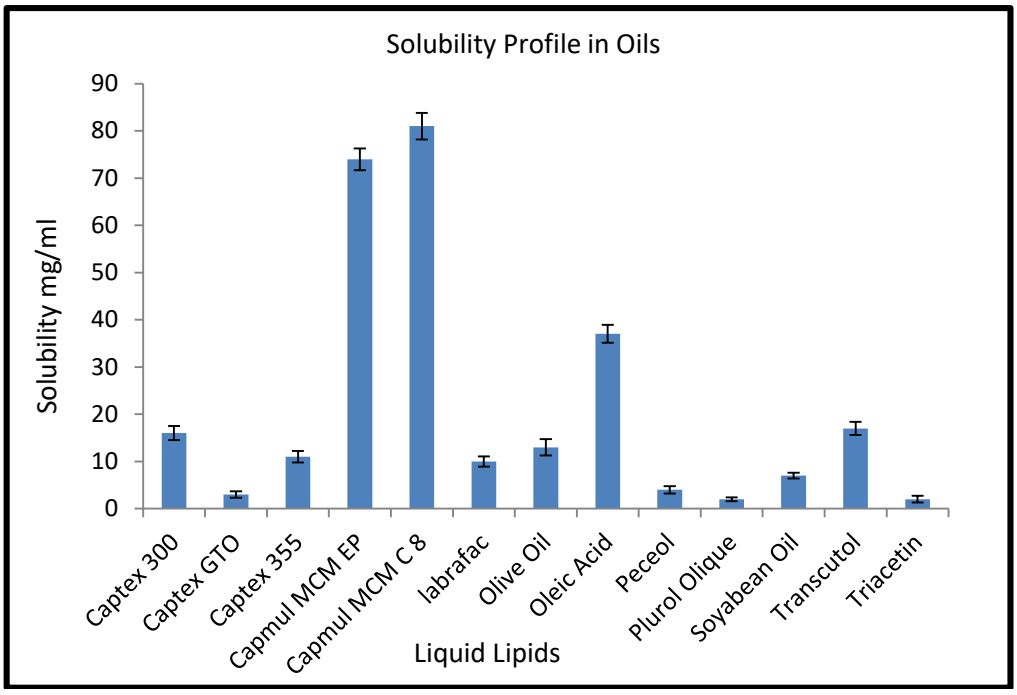

Fig: 5.6- Graphical Presentation of solubility of Rifabutin in Liquid Lipid where Values are mean ±SD; n=3

For the preparation of NLCs, solidg lipid can be shortlisted according to their relative affinity for the drug. Various strategies have been used before for the assurance of solubility of drug in solid lipids. In any case, we have built up another method in light of the guideline of drug partitioning between water and solid lipid (at the temperature above melting point of the lipid) according to their affinity for different phase. Besides, solid lipids were assessed for their physical compatibility with the liquid lipid.

Table: 5.7- Solubility of Rifabutin in Liquid Lipid

Name of Liquid Lipids	Solubility mg/ml
Captex 300	16 ± 1.5
Captex GTO	03±0.7
Captex 355	11 ± 1.2
Capmul MCM EP	74 ± 2.3
Capmul MCM C 8	81 ± 2.8
labrafac	10 ± 1.1
Olive Oil	13 ± 1.7
Oleic Acid	37 ± 1.9
Peceol	04 ± 0.8
Plurol Olique	02 ± 0.4
Soyabean Oil	07 ± 0.6
Transcutol	17 ± 1.4
Triacetin	02 ± 0.7

Values are mean ±SD; n=3

Liquid lipids for the preparation of NLCs were selected depending on their ability of carry the drug. A good affinity of the solid and liquid lipid may warrant for high entrapment efficiency, which is an essential qualification of a carrier system. Hence, Capmul MCM EP and Capmul MCM C-8 can be considered as the best choice for the preparation of NLCs to maximize the encapsulation of drug.

5.4 Solubility of Rifabutin in Different Solid Lipid

Liquid and solid lipids for the preparation of NLCs were selected depending on their ability of carry the drug. A good affinity of the solid lipid may warrant for high entrapment efficiency, which is an essential qualification of a carrier system. Good solubility of rifabutin was observed in Precirole ATO-5, Compritol ATO 888, Gelucire 39/01. However, Precirole ATO-5 showed highest solubility for rifabutin, i.e. 83 ± 2.6 mg/mL, 75 ± 2.6 mg/mL, 72 ± 2.4 mg/mL (Kakkar, et al., 2011).

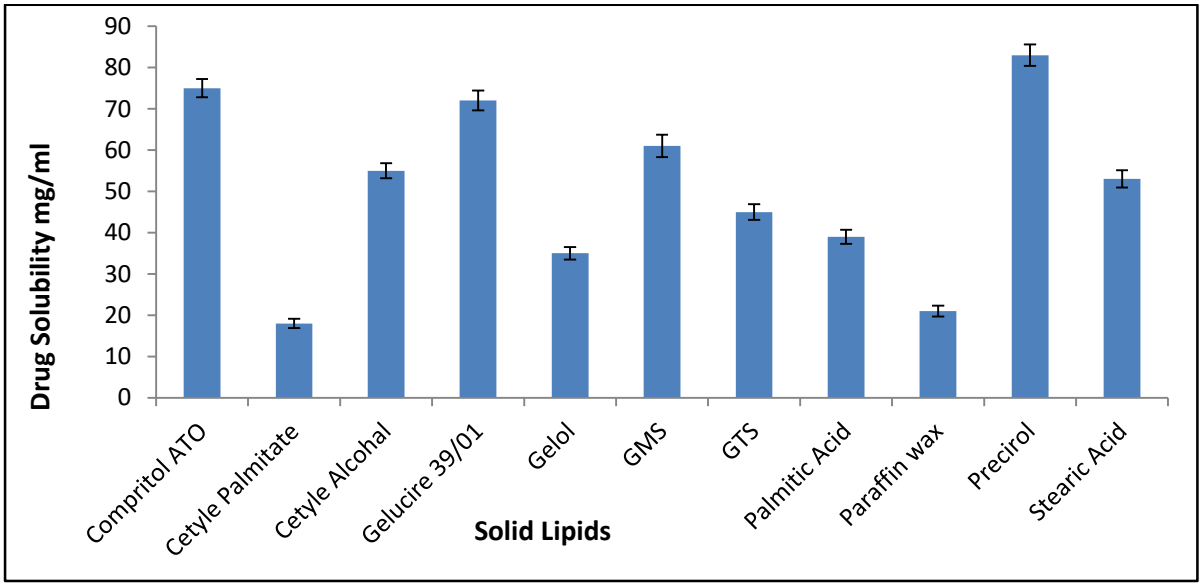

Fig: 5.7- Graphical Presentation of solubility of Rifabutin in Solid Lipid where Values are mean ±SD; n=3

Due to high affinity Rifabutin could be considered as the ingredient for the preparation of NLCs. All three shortlisted solid lipids were further evaluated for the physical compatibility with capmul mcm C-8 and capmul mcm EP. Gelucire 39/01 and Compitrol ATO-888 failed to congeal at room temperature. Such an observation could be attributed to the decrease in combined melting temperature for the lipid mix. On the other hand, no separation was observed in the congealed mass of Precirol ATO-5. However, on microscopic examination Precirol ATO-5 mix was found to have good miscibility, whereas compritol mix showed a uniform smear. Therefore based on the affinity of the lipids for rifabutin and

physical compatibility, capmul mcm C-8, capmul mcm EP and Precirol ATO-5 were selected as liquid and solid lipids, respectively.

Table: 5.8- Solubility of Rifabutin in Lipid

Name of Liquid Lipids	Solubility mg/ml
Compritol ATO	75 ± 2.2
Cetyle Palmitate	18 ± 1.1
Cetyle Alcohal	55 ± 1.8
Gelucire 39/01	72 ± 2.4
Gelol	35 ± 1.5
GMS	61 ± 2.7
GTS	45 ± 1.9
Palmitic Acid	39 ± 1.7
Paraffin wax	21 ± 1.3
Precirol	83 ± 2.6
Stearic Acid	53 ± 2.1

Since, one of three lipids with highest affinity for the drug was found to have good compatibility for the selected oil phase; the other lipids were not evaluated for further development of formulation.

5.4.1 Affinity Study

According to their affinity between different phases of Lipids. Besides, solid lipids were assessed for their physical compatibility with the liquid lipid. Drug was determined in solid lipid solution and in water as well. Microscopically visualised and evaluated shown in figure given below (Gaspar, et al., 2000).

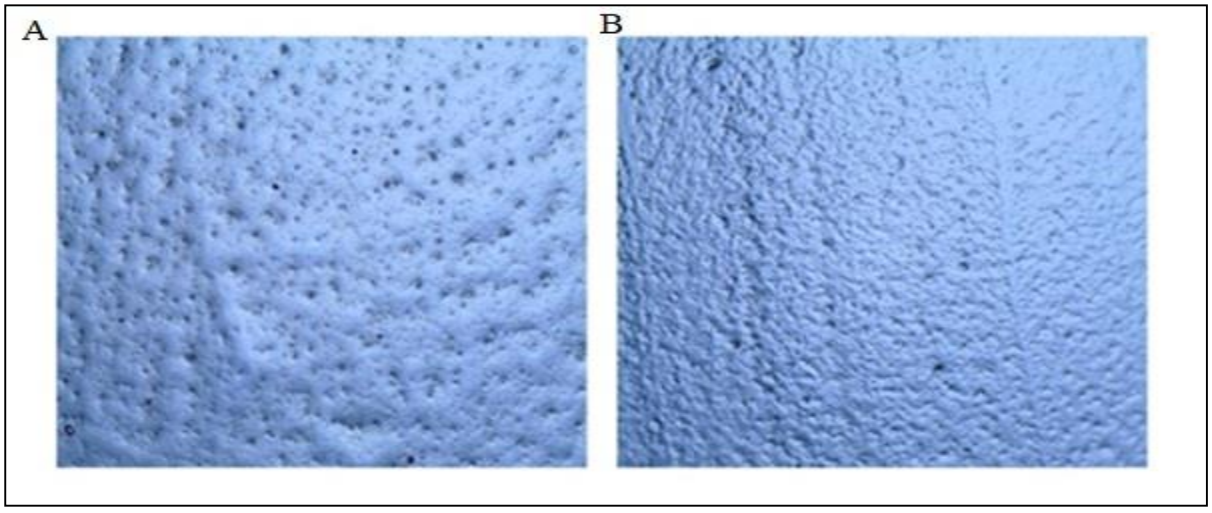

Figure: 5.8- Microscopic evaluation of oil and solid lipid mix smear where Fig A. Precirol ATO-5 with Capmul MCM C-8 and B. Precirole ATO-5 with Capmul MCM EP

5.5 Selection of liquid–solid lipid ratio

Liquid–solid lipid ratio was selected with the intention to have good drug carrying capacity with proper melting point to maintain the solid/semisolid consistency of the particles at room temperature. As capmul MCM C-8 and capmul MCM EP was observed to have better drug solubilization capacity, a higher ratio of liquid lipid could be useful for the higher drug entrapment. However, at the same time the consistency of the lipid mix cannot be compromised. It was observed that the liquid–solid lipid mixture in the ratio up to 60:40 were having sufficient melting point (60–65^{0}C). On further increase of oil content, the melting point of the mixture was below desired level. Hence 60:40 was selected as the working ratio for the liquid–solid lipid mixture for the higher drug entrapment. (Nirbhavane, et al.,2017).

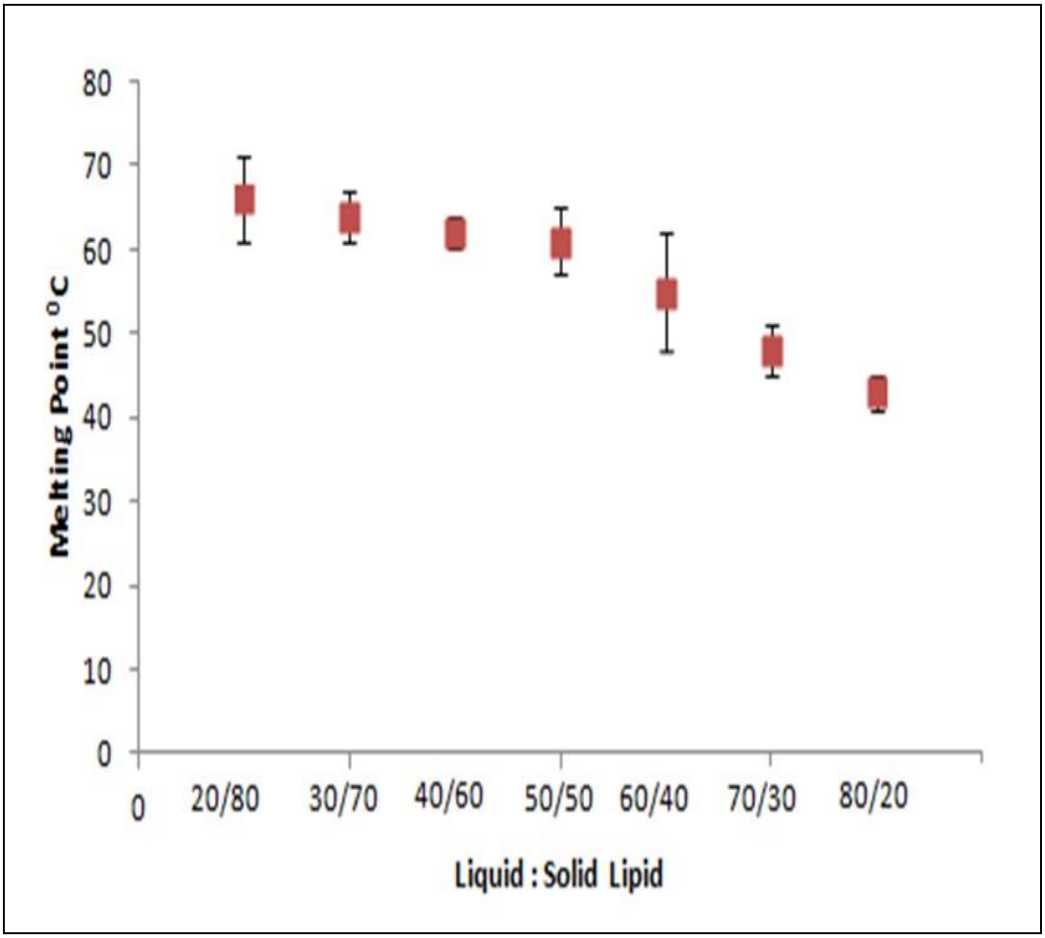

Figure: 5.9- Selection of Solid Lipid Ratio for Capmul MCM C-8 and Capmul MCM EP with Precirol ATO-5

5.6 Selection of surfactant

The emulsification capability was considered as the criteria of the selection of the surfactants. A higher percentage transmittance corresponds to the smaller sized particles and hence better

emulsification. It was found that Poloxmar-188 produced an emulsion with the highest percentage transmittance for the system in comparison to the other surfactants. However, other surfactants such as Pluronic F-68 and Labrasol were also found to have good emulsification capability for the lipid mix. In this study Poloxmar-188 selected as a surfactant with good emulsification properties.

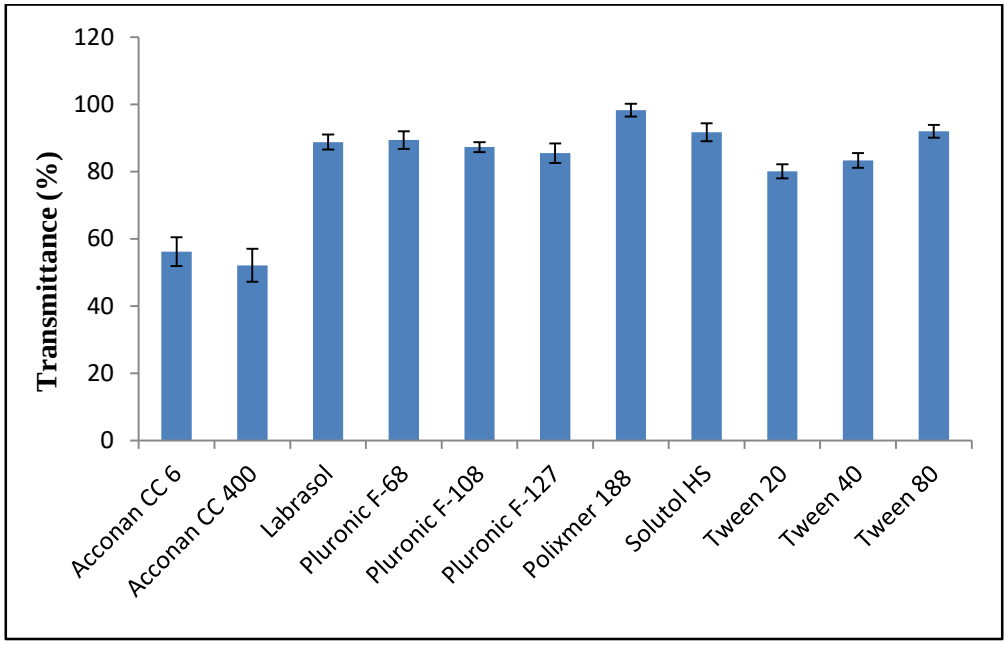

Figure: 5.10- Selection of Surfactant on Percentage Transmittance

The emulsification ability was considered as the criteria of the selection of the surfactants. A higher rate of transmittance relates to the smaller sized particles and hence better emulsification. It was found that Poloxamer-188 created an emulsion with the most percentage rate of transmittance for the system in-comparison to alternate surfactants.

Table: 5.9- Percentage Transmittance of Surfactant with SD (n=3)

S. No	Name of Surfactant	Transmittance (%) ± SD
1	Acconan CC 6	56.2 ± 4.3
2	Acconan CC 400	52.1 ± 4.9
3	Labrasol	88.8 ± 2.2
4	Pluronic F-68	89.4 ± 2.6
5	Pluronic F-108	87.3 ± 1.5
6	Pluronic F-127	85.5 ± 2.9
7	Polixmer 188	98.3 ± 1.9
8	Solutol HS	91.7 ± 2.7
9	Tween 20	80.1 ± 2.1
10	Tween 40	83.3 ± 2.2
11	Tween 80	92 ± 1.9

However, other surfactants, for example, Labrasol and Pluronic F-68 were additionally found to have great emulsification capacity but mild toxic potential for the lipid blend. In such a circumstance a surfactant with great emulsification properties can likewise be chosen on the bases of its extra advantages. In present case Polixmer 188 was found to have some other extra advantages over nearly challenging surfactants. Polixmer 188 is strong in nature so it is probably going to have no toxic effect over the dissolving purpose of last NLCs and subsequently it is a decent decision to evade supercooled melt issue later on. Hence, Polixmer 188 was selected as the main surfactant for the system. It was observed from the past reviews that a combination of surfactant is always better to create small size Nano Lipid Carrier (NLC)s with better storage stability (Sánchez-López, et al., 2017).

5.7 Preparation of Nanostructure Lipid Carriers of Rifabutin

NLC's were chosen to be prepared by Solvent Injection technique developed by (Muller et al, 2002) based on literature review. Although several process and formulation parameters were changed batch to batch but general procedure is outlined here. 5mg of Rifabutin was weighed and dissolved using bath sonicator in liquid lipid (µl) taken in a 25 ml beaker. To it weighed amount of solid lipid (mg) was added and also measured ml of acetone (ml). Total lipid concentration was maintained constant at 1%w/w.

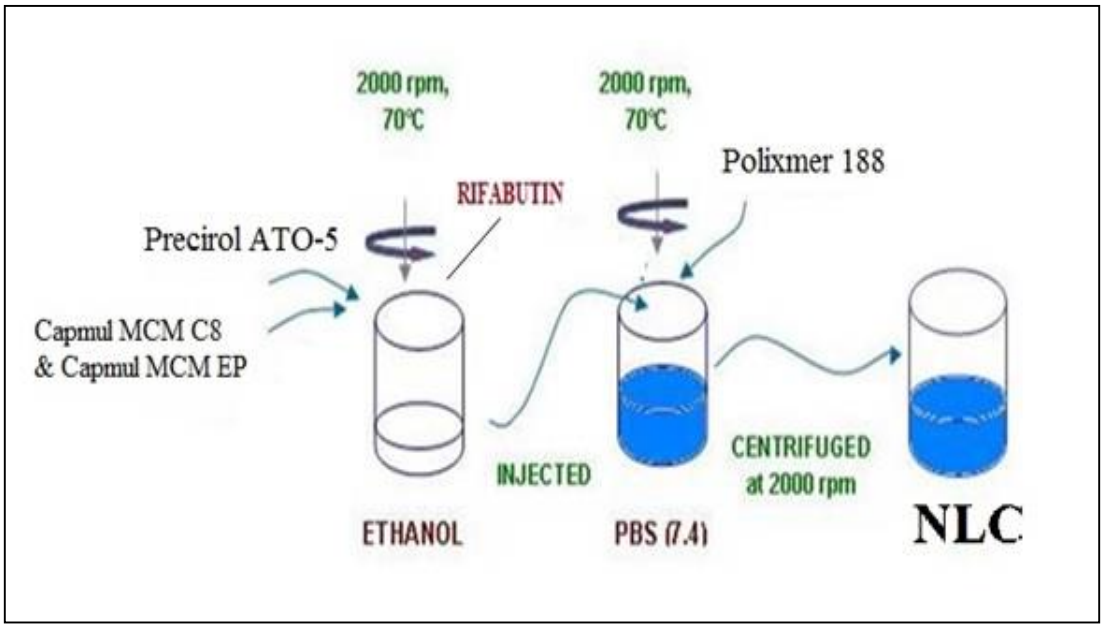

Fig:5.11- Diagrammatic presentation of NLC Method for formulation Preparation

The beaker was covered tightly with an aluminum foil and sonicated in a pre-heated bath sonicator or about 2 min. Parallely 20 ml of poloxamer 188 solution (1.5%w/w) was pipetted

into a 50 ml beaker and heated to 80ºC on a hot plate placed under a IKA T25 disperser (off mode). The hot acetone solution (~38ºC) was withdrawn into a 6ml syringe and disperser turned on. The acetone solution was added dropwise to the poloxamer solution stirred constantly at 10,000/15,000 rpm. The procedure was executed as directed by design of experiment. The formed pre-emulsion was cooled for about 2 minutes prior to sonication using UP200H sonicator. The formed nanoformulation was filtered prior to storage (Almeida, et al., 2017).

5.7.1 Encapsulation efficiency of Nano Lipid Carrier (NLC)

Encapsulation efficiency of Nano Lipid Carrier (NLC) was calculated with the help of Nanosep method. A known dilution of the NLC was prepared and 500µl of it was transferred to the upper chamber of Nanosep® centrifuge tubes fitted with an ultrafilter. The Nanosep® was centrifuged at 15,000 rpm for 20 mins. The filtrate was diluted appropriately and the amount of drug in the phase was determined using UV spectroscopy analysis at 242 nm (Puglia, et al., 2017). The entrapment efficiency was calculated by the following equation:

$$\text{Drug E.E. (\%)} = \frac{\text{Total drug content-Free drug content}}{\text{Total drug content}} \times 100$$

Total drug content = conc. obtained × dilution factor × Volume of formulation

5.7.2 Screening and Optimization for Formulation One

A conventional optimization method requires a large number of trials with low sensitivity, while other sophisticated design tools can increase the sensitivity of the optimization but the number of trials still remains high. Conventional optimization methods lack precision and single design tools lack the efficiency to reduce the number of trials in the case of a large number of variables.

This work a logical combination of different optimization tools (PBD and Box Benhekan) was successfully used to reduce the total number of trials and hence eliminate the unnecessary waste of resources and time.

The stepwise combination of design tools not only helped in reducing the number of trials but also increased our understanding about the effects of different variables and the interactions between different variables on the characteristics of the NLCs. Hence, the

rational combination of design methods used in this study was proved to be more efficient and logical in optimization of formulations (Rizwanullah, et al., 2017).s

5.8 Process of Screening through Plackett-Burman Design (PB)

In the process of Screening and Optimisation can evaluate how the regression tool in Mintab-17, intended for response surface methods (RSM), for this work with such happenstance variables if there's any possibility of performing a designed experiment. Highly Fractionated experiment makes good building blocks for sequential experiments. Many researches use Plackett-Burman design for this purpose by Minitab-17 software. In this work, I confounded in the interpretation of effects from these low-resolution designs. The main effect may be aliased with plausible two factor interactions. If this occurs, we might be able to eliminate the confounding by running further experiments using a fold over design. This technique adds further fractions to the original design matrix (Singh, et al., 2017).

Table: 5.10- Randomized Design Table of selected factors with its Response

S. No	Temperature	Needle Size	Injection Speed	Homogenization time	Homogenization Speed	Sonication time	Drug Lipid Ratio	Solid Lipid & Liquid Lipid Ratio	Poloxamer 188	Organic & Aqueous Ratio	Particle Size	Entrapment Efficiency
1	40	16	5	10	10000	1	1	1	1	1	177	55
2	70	16	10	10	10000	1	1.5	1.5	2	1	193	61
3	70	16	5	10	15000	1.25	1.5	1	2	5	146	62
4	70	16	10	30	10000	1.25	1	1	1	5	131	51
5	40	31.5	10	30	10000	1.25	1.5	1	2	1	144	67
6	40	16	5	30	15000	1.25	1	1.5	2	1	199	60
7	40	31.5	5	10	10000	1.25	1.5	1.5	1	5	296	62
8	70	31.5	10	10	15000	1.25	1	1.5	1	1	321	49
9	70	31.5	5	30	15000	1	1.5	1	1	1	144	64
10	40	16	10	30	15000	1	1.5	1.5	1	5	111	61
11	40	31.5	10	10	15000	1	1	1	2	5	139	64
12	70	31.5	5	30	10000	1	1	1.5	2	5	177	66

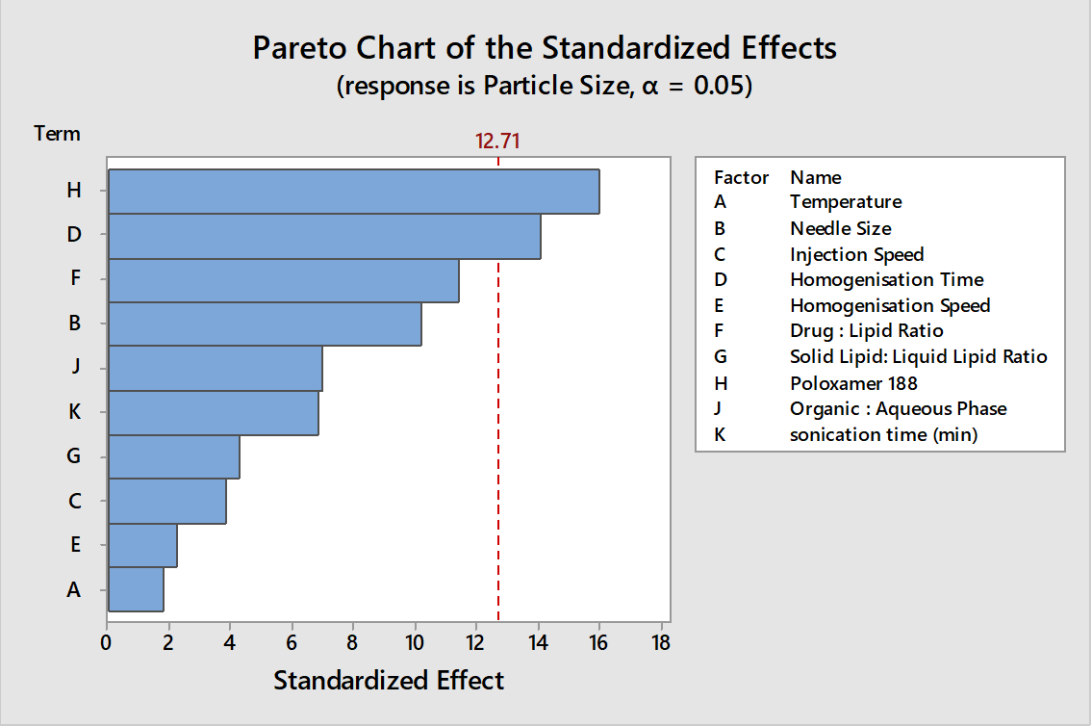

Fig: 5.12- Showing response on Particle size of significant factors through Pareto chart

Particle Size = -71.6 + 0.256 Temperature + 2.839 Needle Size - 3.333 Injection Speed -3.050 Homogenisation Time - 0.001933 Homogenisation Speed + 197.3 Drug : Lipid Ratio - 36.67 Solid Lipid: Liquid Lipid Ratio + 138.67 Poloxamer 188 - 30.33 Organic : Aqueous Phase - 7.42 sonication time (min)

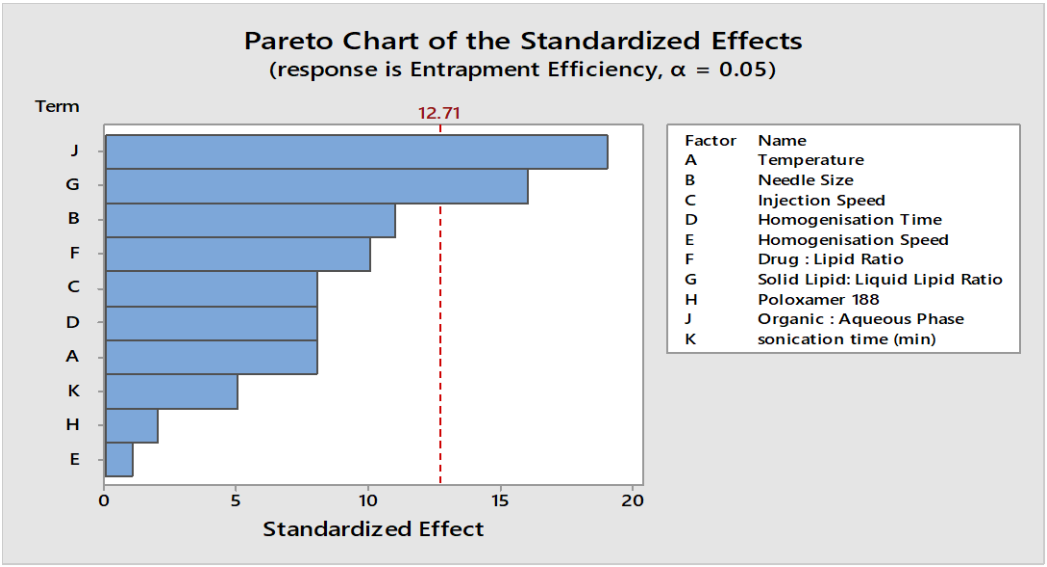

Fig: 5.13- Showing significant factors response on Entrapment Efficiency through Pareto chart

Entrapment Efficiency = 54.19 - 0.0889 Temperature + 0.2366 Needle Size - 0.5333 Injection Speed + 0.1333 Homogenisation Time - 0.000067 Homogenisation Speed - 13.33 Drug : Lipid Ratio + 10.667 Solid Lipid: Liquid Lipid Ratio -1.333 Poloxamer 188 + 6.333 Organic : Aqueous Phase + 0.4167 sonication time (min)

5.8.1 Effect of Process design variables on responses for formulation One

5.8.1.1 Effect on particle size

Particle size as indicated by the Box-Behnken design has been most profusely affected by sonication time as expressed in literature itself. Homogenisation time supplies energy intensively to the formulation leading to aggressive cavitations which leads to overall increase in surface area. The supplied power in stored in the formulation as surface energy which is directly proportional to total surface area.

Therefore it undoubtedly shows maximum effect on the particle size. This principle is clearly reflected in the data for as we move from run 1 to run 2, other 3 factors are being held constant and particle size clearly decreases from 198.9±31.6 nm to 111.9±12.3 nm as we move from homogenisation time of 5 minutes to 10 minutes (Sahu, et al., 2017).

Table: 5.11- Process of Optimisation through Box-Behnken Design

S.No	Homogenization Time	Poloxamer 188	Organic: Aqueous Ratio	Solid Lipid: Liquid Lipid Ratio	Particle Size	Entrapment Efficiency
1	20	1.25	2	1.5	144	63
2	20	1.5	2	1.25	163	68
3	10	1.25	1.5	1.5	198	45
4	30	1.5	1.5	1.25	111	48
5	20	1	1	1.25	156	57
6	20	1	1.5	1	198	44
7	10	1.25	1.5	1	189	66
8	20	1	1.5	1.5	168	44
9	20	1.5	1.5	1.5	157	38

10	20	1.25	1	1.5	146	44
11	30	1.25	1.5	1	110	48
12	30	1	1.5	1.25	115	52
13	30	1.25	1.5	1.5	125	74
14	10	1	1.5	1.25	198	48
15	20	1	2	1.25	189	72
16	10	1.25	2	1.25	108	68
17	20	1.5	1.5	1	100	61
18	20	1.25	2	1	171	78
19	30	1.25	1	1.25	132	43
20	30	1.25	2	1.25	111	73
21	20	1.5	1	1.25	168	51
22	20	1.25	1	1	151	64
23	10	1.25	1	1.25	199	52
24	20	1.25	1.5	1.25	169	59
25	20	1.25	1.5	1.25	133	58
26	10	1.5	1.5	1.25	121	61
27	20	1.25	1.5	1.25	176	55

Similar observations can be made with rest of the readings too. As indicated by design an increase of Homogenisation time from 10 min to 20 minutes results in averaged 55 nm decreases in particle size which sure is significant. Moreover tests of significance i.e. Anova indicates thus as well (Anand, et al., 2017).

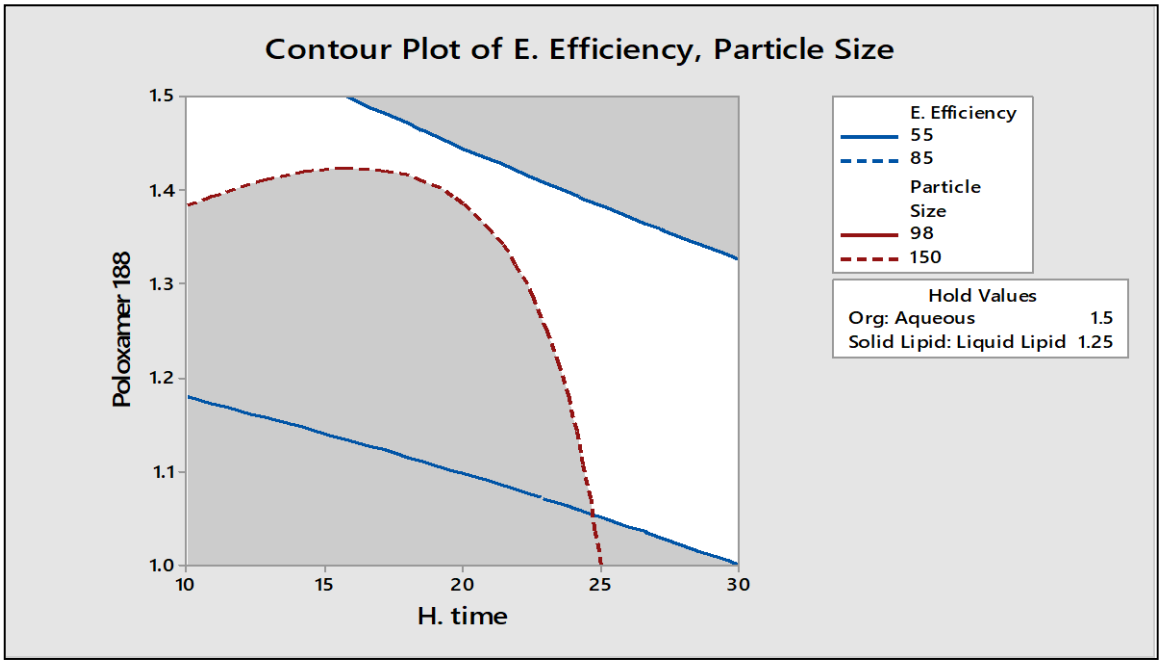

Fig: 5.14- Showing optimisation of entrapment efficiency and Particle size on the value of Poloxamer 188 and Homogenization time

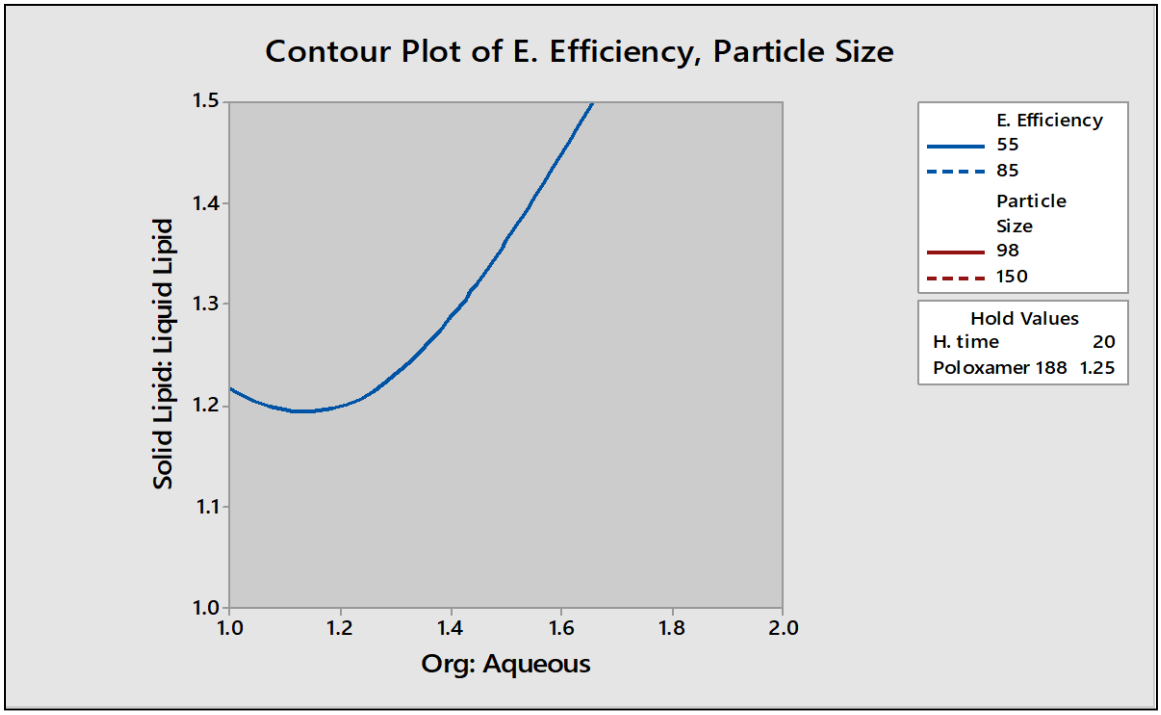

Fig: 5.15- Showing optimisation of entrapment efficiency and Particle size on the value of Ratio of Solid Lipid & liquid Lipid and Organic Phase & Aqueous Phase

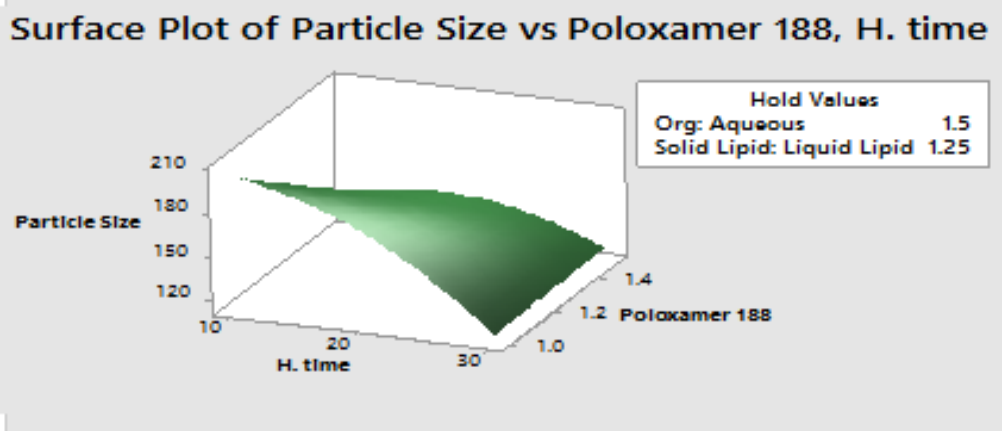

Fig: 5.16- Showing the effect of Particle size vs Poloxamar 188, Homogenization time

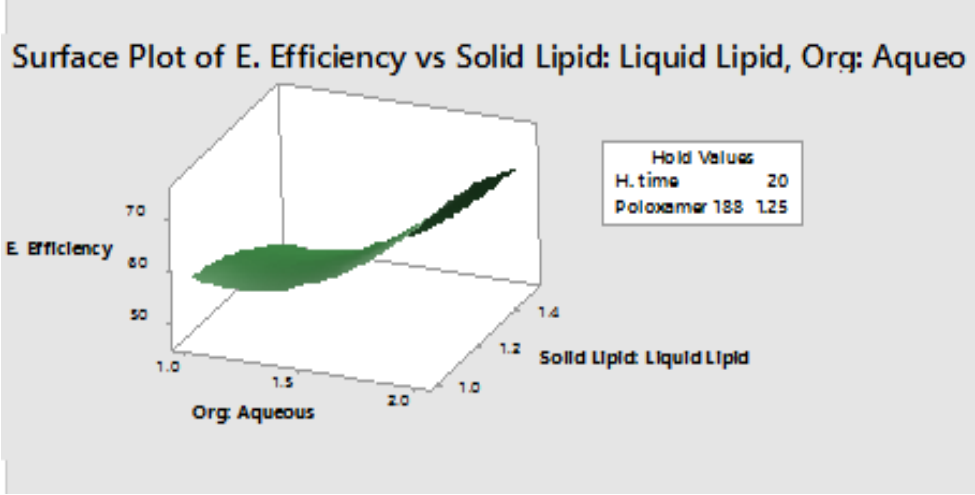

Fig: 5.17- Showing the effect of Entrapment Efficiency vs Solid Lipid: Liquid Lipid and the Ratio of Organic Phase & Aqueous Phase

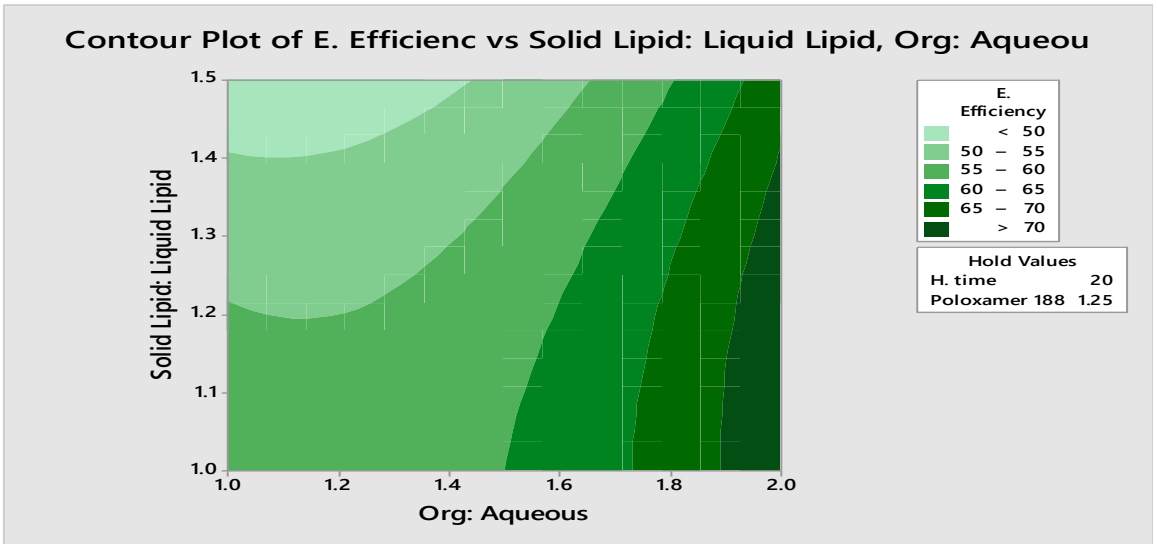

Fig: 5.18- Showing the effect of Entrapment Efficiency vs Solid Lipid: Liquid Lipid and the Ratio of Organic Phase & Aqueous Phase through contour Plot

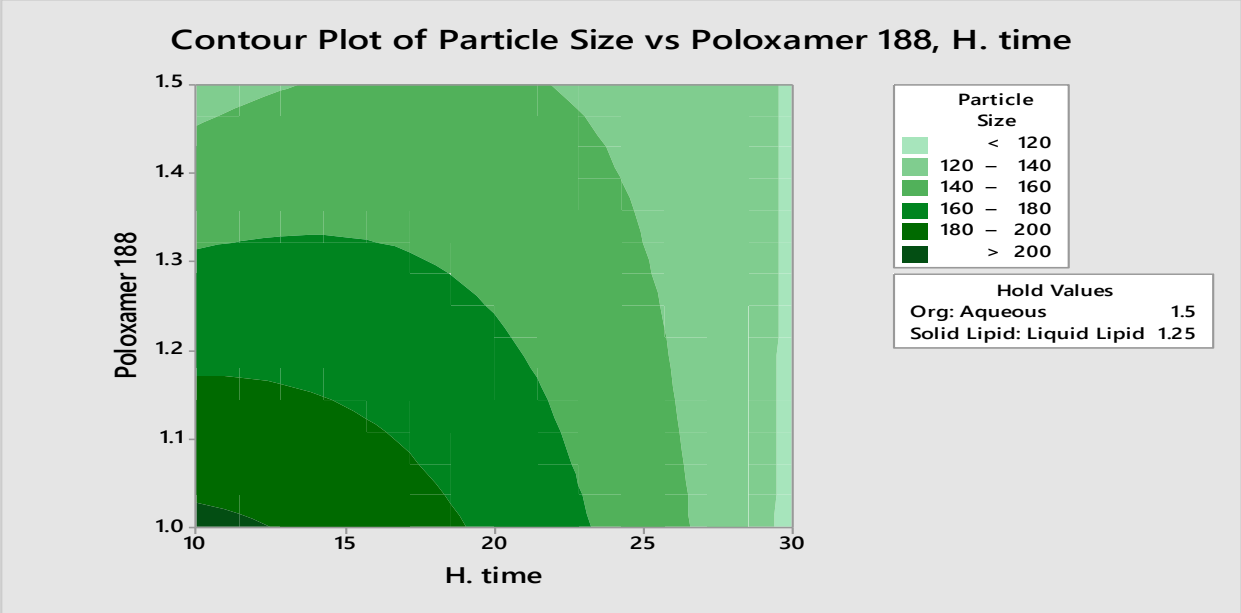

Fig: 5.19- Showing the effect of Particle size vs Poloxamar 188, Homogenization time through Contour Plot

The optimized NLC with Capmul EP needed to qualify the criteria of high entrapment efficiency, low particle size.

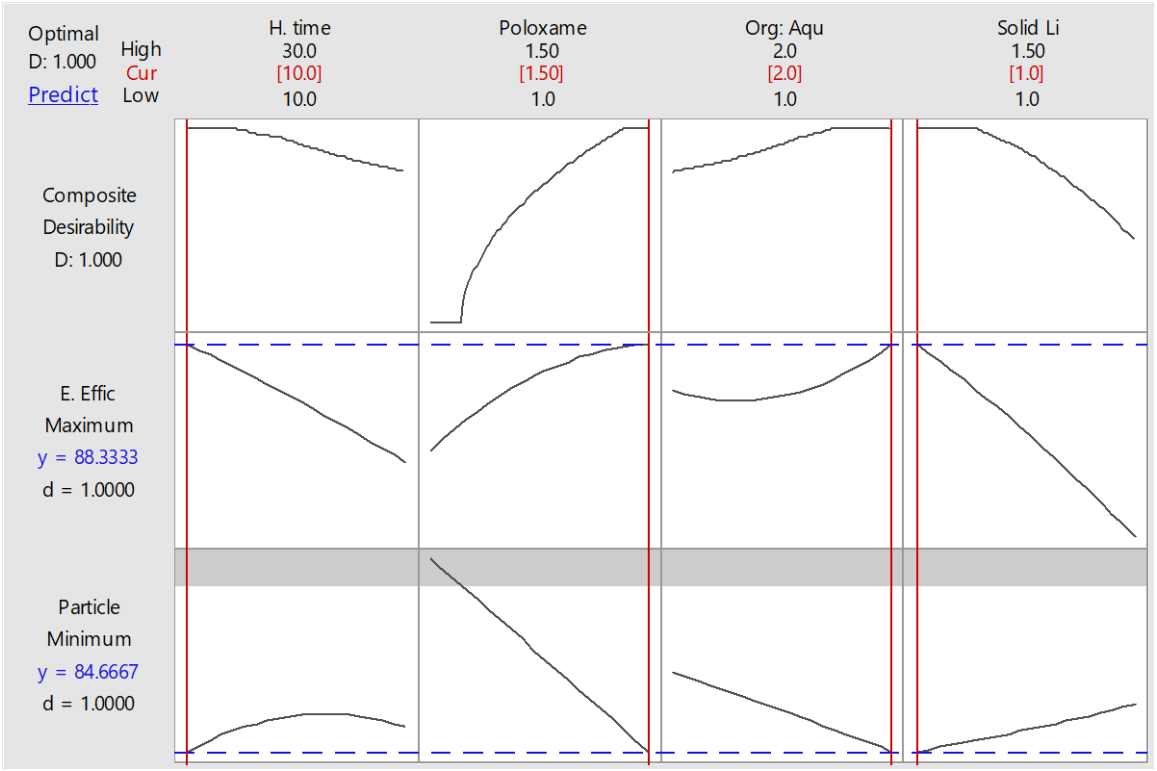

Fig: 5.20- Showing the effect of factors on response through response optimizer

Determined value of optimised factors is given below:

Homogenisation time (min.)- (10), Poloxamer 188- (1.5%), Org: Aqueous- (2.0%), Solid Lipid: Liquid Lipid- (1.0%) these values are used for the further study for preparation of NLC containing rifabutin.

5.8.1.2 Effect of Process design variables on responses for formulation Two

After screening and setting values of process parameters at optimum levels calculated batches with rifabutin were prepared according to central composite design. 27 runs, all in triplicate were executed and mean responses calculated (Beg, et al., 2017).

For NLC optimization 04 factors and 2 response variables were chosen with factors set at 3 different levels. The selection of factors was done based on screening.

Table: 5.12- Process of Optimisation through Box-Behnken Design

Homogenisation time (min)	Poloxamer 188	Organic : Aqueous Ratio	Solid : Liquid Lipid Ratio	Particle Size	E. Efficiency
17.5	1.25	1	1	144	59
17.5	1.5	2	1.25	163	61
17.5	1.25	1.5	1.25	172	54
25	1	1.5	1.25	111	52
17.5	1.25	1.5	1.25	156	57
17.5	1.25	2	1	165	60
17.5	1.25	1	1.5	159	48
10	1.5	1.5	1.25	198	51
25	1.25	1.5	1.5	112	49
17.5	1	1.5	1	146	53
17.5	1.5	1	1.25	110	48
17.5	1	1.5	1.5	115	52
10	1.25	1.5	1	201	74
25	1.5	1.5	1.25	121	48
17.5	1.5	1.5	1.5	176	63
25	1.25	1.5	1	108	68
25	1.25	2	1.25	100	61
17.5	1.5	1.5	1	171	78
10	1.25	1	1.25	132	43
10	1	1.5	1.25	111	56
17.5	1.25	2	1.5	168	61
25	1.25	1	1.25	151	54
10	1.25	2	1.25	199	70
10	1.25	1.5	1.5	169	55
17.5	1.25	1.5	1.25	133	58
17.5	1	2	1.25	121	52
17.5	1	1	1.25	176	51

For lipid ratio coding was done of values for easier calculation as indicated in table above. The responses obtained are in graphically as follows:

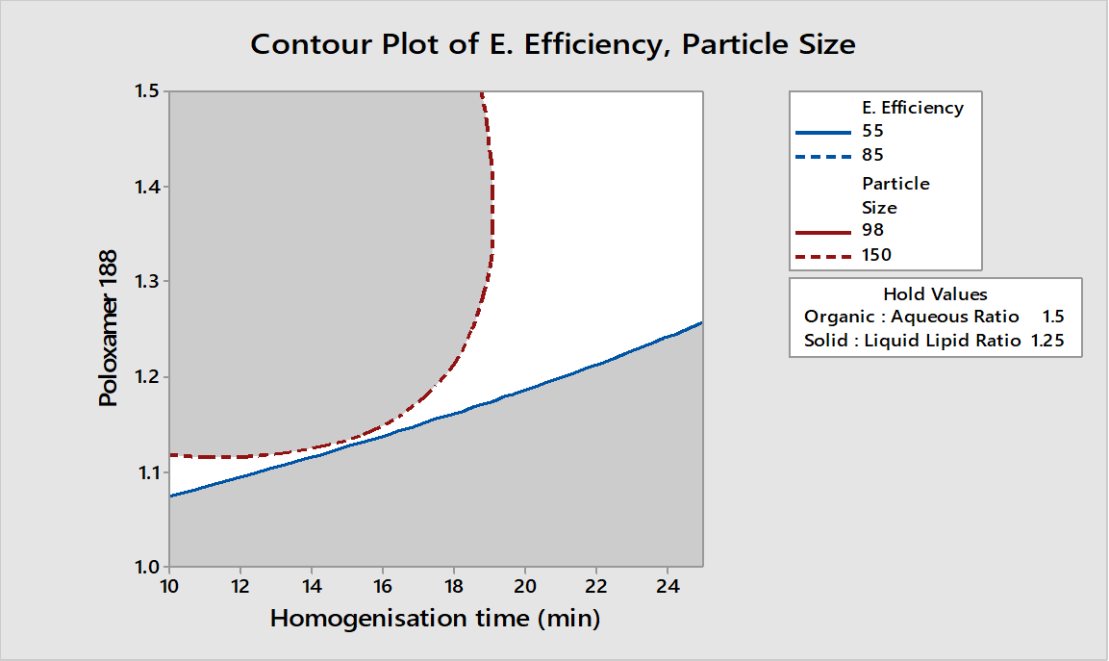

Fig: 5.21- Showing optimisation of entrapment efficiency and Particle size with the value of Poloxamer 188 and Homogenization time for Formulation Two

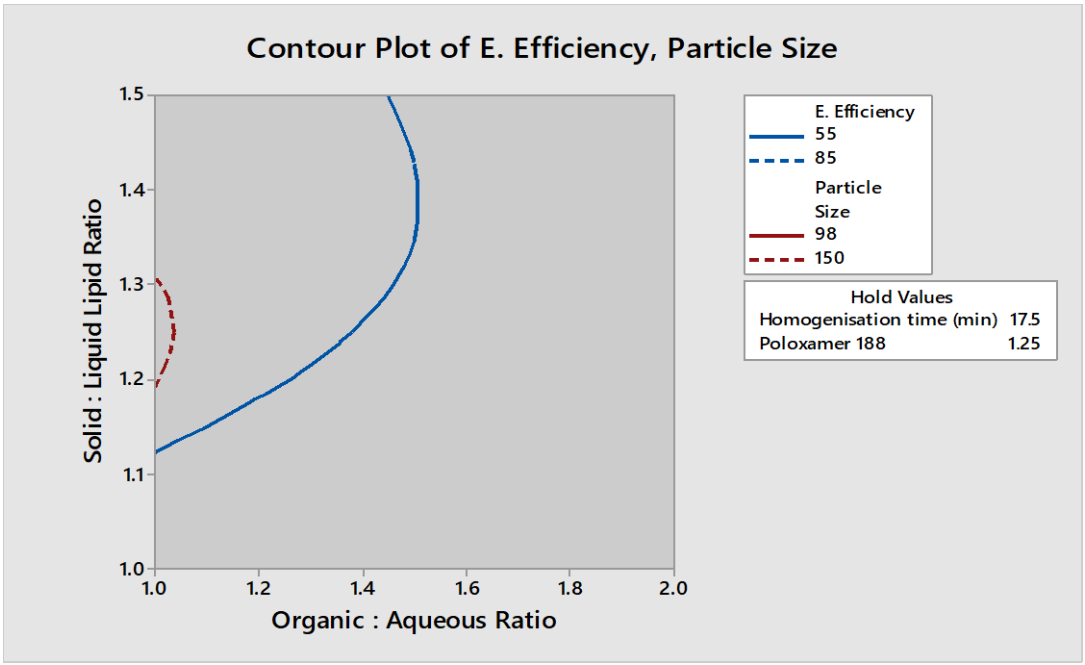

Fig: 5.22- Showing optimisation of entrapment efficiency and Particle size with the value of Solid Liquid Lipid Ratio for Formulation Two

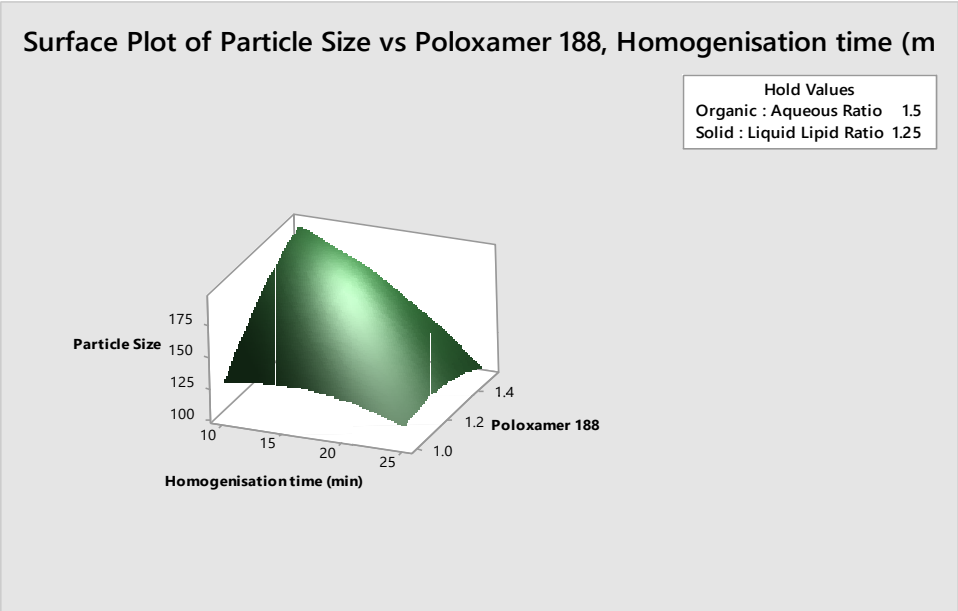

Fig: 5.23- Surface Plot of Particle size vs Poloxamer 188, Homogenization Time

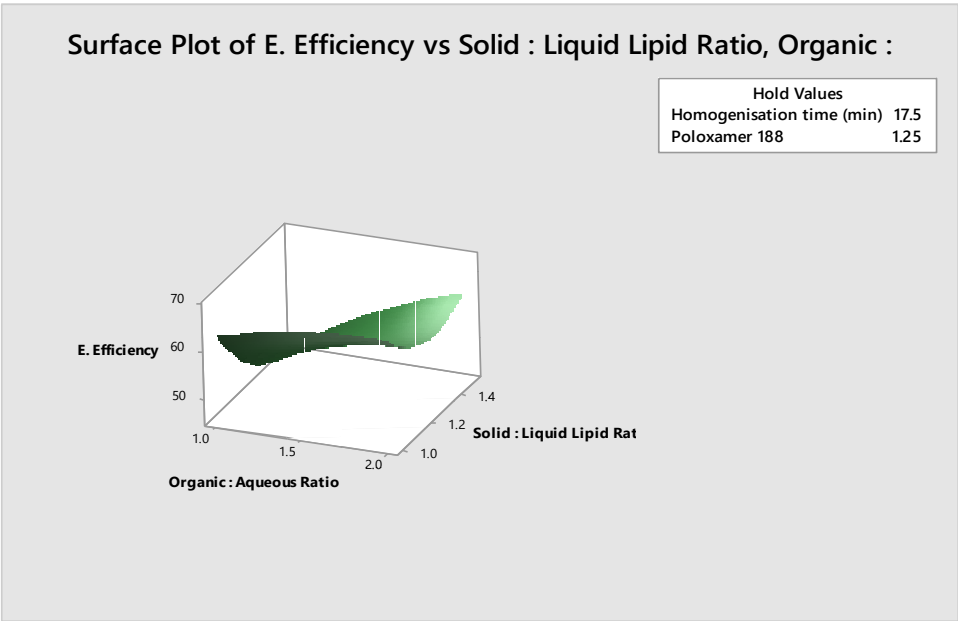

Fig: 5.24- Surface Plot of Entrapment Efficiency vs Solid, Liquid Lipid Ratio and Organic Aqueous Phase

Entrapment efficiency is increases while increasing the Aqueous Ratio & Organic Ratio. After that particle size is increases when increasing the solid lipid ratio.

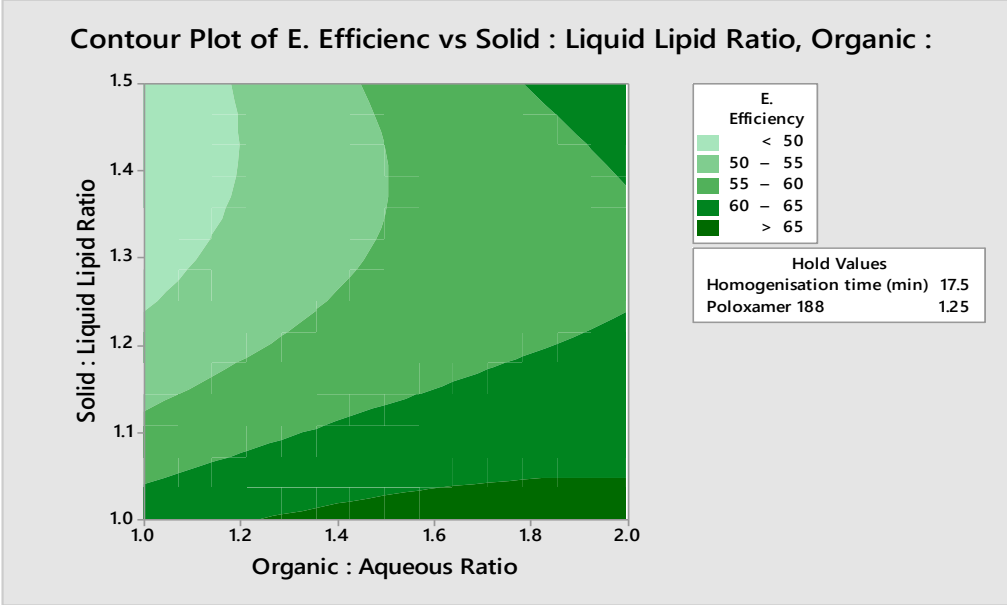

Fig: 5.25- Showing the effect of Entrapment Efficiency vs Solid Lipid: Liquid Lipid and the Ratio of Organic Phase & Aqueous Phase through contour Plot

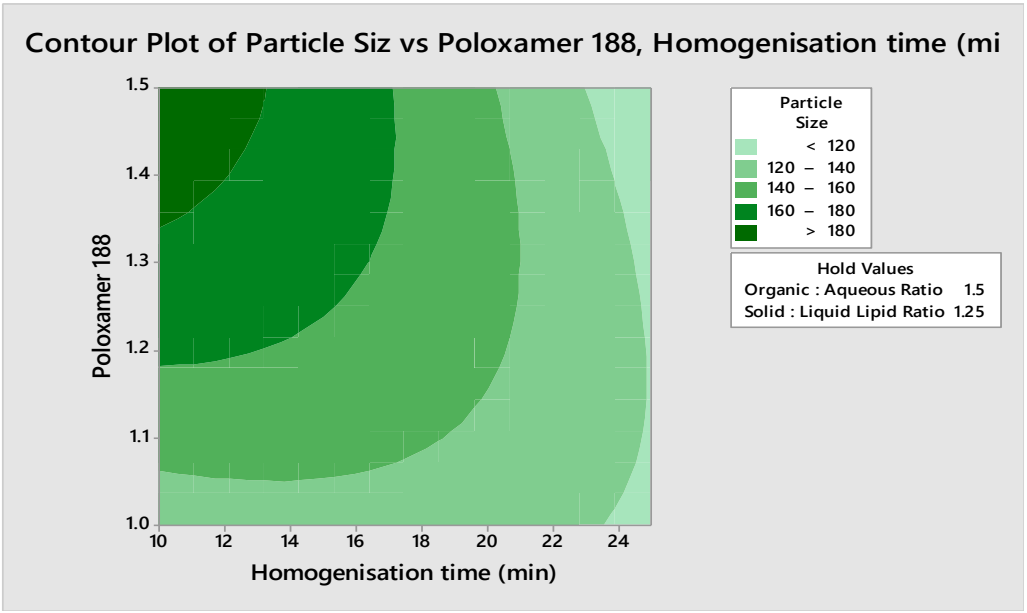

Fig: 5.26- Showing the effect of Particle size vs Poloxamar 188, Homogenization time through Contour Plot

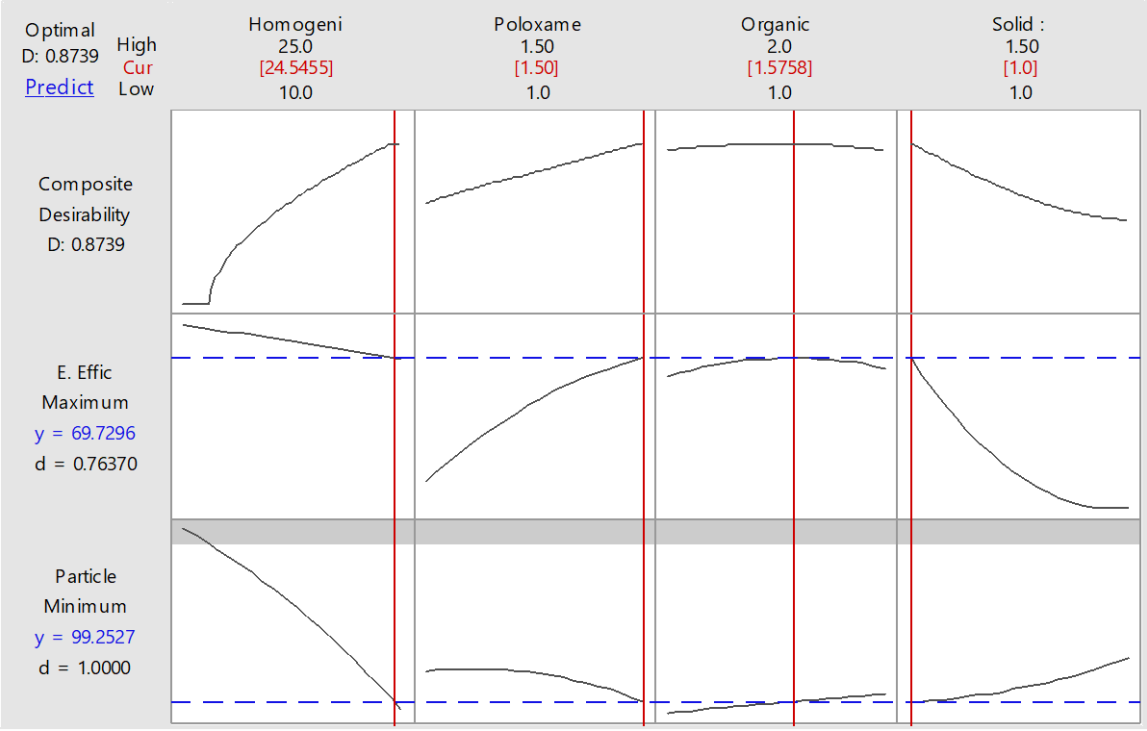

Fig: 5.27- Showing the effect of factors on response through response optimizer

The optimized NLC Capmul EP needed to qualify the criteria of high entrapment efficiency, low particle size. The determined value of optimised factors is given below:

Homogenisation time (min.)- (24.5), Poloxamer 188- (1.5%), Org: Aqueous- (1.5%), Solid Lipid: Liquid Lipid- (1.0%) these values are used for the further study for preparation of NLC containing rifabutin (Bhise, et al., 2017).

5.9 Optimization parameters

Optimization parameters were kept similar for both the preparations, temperatures before 1st and 2nd desolvation step, pH before 2nd desolvation step, speed of desolvating agent addition, stirring speed of the reaction and the ratio of the crosslinking agent added with the drug and polymer. The optimization parameters impart significant effect on the Nano Lipid Carrier (NLC) preparation hence were carefully monitored.

5.9.1 Characterization

The characterization of Rifabutin loaded NLC was performed by employing various analytical techniques to ascertain studies to confirm complete entrapment of the drug within the lipid, particle morphology by Scanning Electron Microscopy, Transmission Electron Microscopy and zeta potential determined (Almeida, et al., 2017).

5.9.1.1 Scanning Electron Microscopy (SEM)

The SEM images of the prepared NLC displayed virtually globular smooth surface. The presence of any perforation or roughness might have been caused due to the evaporation of the desolvating agent (acetone). The morphology of the NLC depends majorly on the amount of the solid lipid agent as it prevents the *in situ* formed NLCs from disintegration. The developed NLC were spherical in shape with smooth, slightly perforated surface as shown in SEM micrographs.

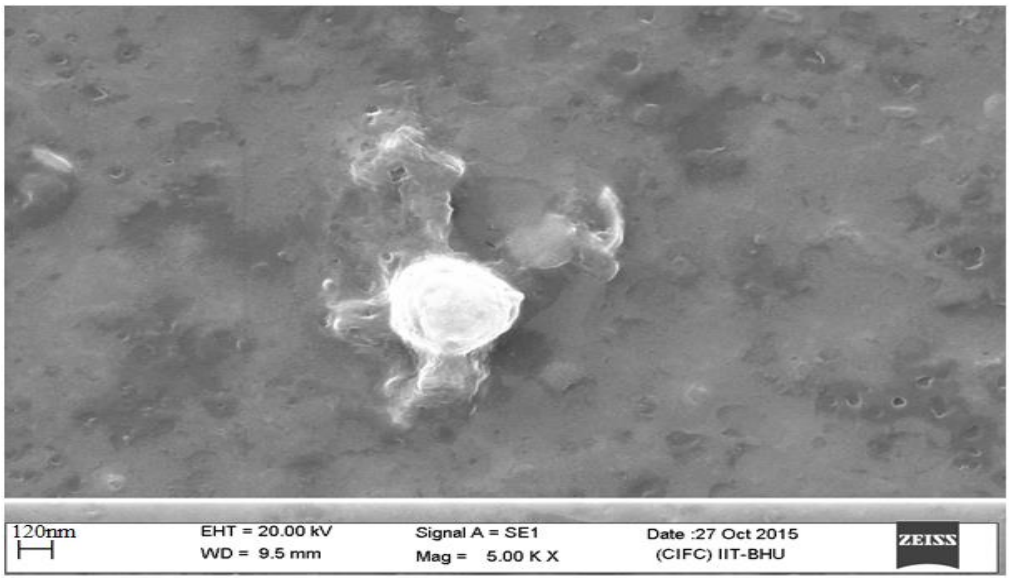

Fig: 5.28- the Scanning Electron Microscopy (SEM) Image of NLC containing Rifabutin

5.9.1.2 Transmission Electron Microscopy (TEM)

The TEM images of the optimized batches of **NLC Capmul mcm C-8** revealed solid, consistent and spherical surfaced nanostructures. The TEM images of the final batche, **NLC Capmul mcm C-8** confirm the size range with the SEM micrographs that the particles were of nanometer range.

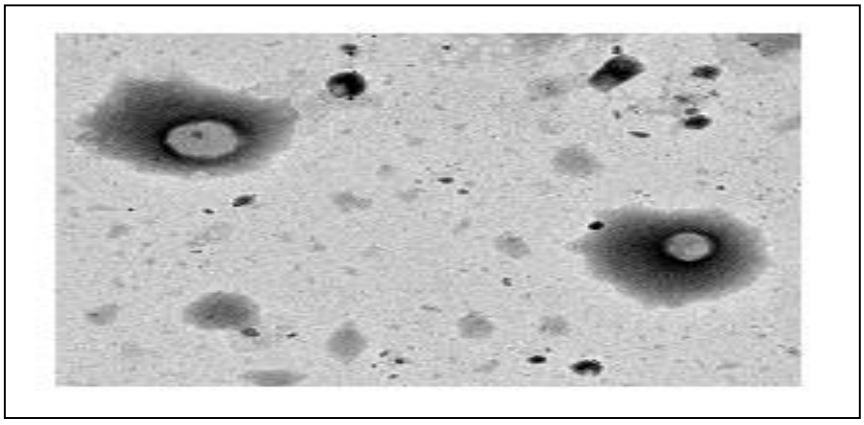

Fig: 5.29- the Transmission Electron Microscopy (TEM) Image of NLC containing Rifabutin

5.9.1.3 *In vitro* drug release study

The dialysis bag diffusion technique was used to study the in- vitro drug release of Rifabutin formulation. 01 ml of Rifabutin NLC Preparation was placed in the dialysis bag (cellulose membrane, molecular weight cut off 12,000) hermetically sealed and immersed into 50 ml of phosphate Buffer Saline (pH 7.4). The entire system was kept at 37 ± 0.5 °C with continuous magnetic stirring at 200 rpm/min. Samples were withdrawn from the receptor compartment at predetermined time intervals and replaced by fresh medium. The amount of drug dissolved was determined with UV spectrophotometer at 242 nm after using the software PSP Dissolution version 3.0 (Nagaich, et al., 2016).

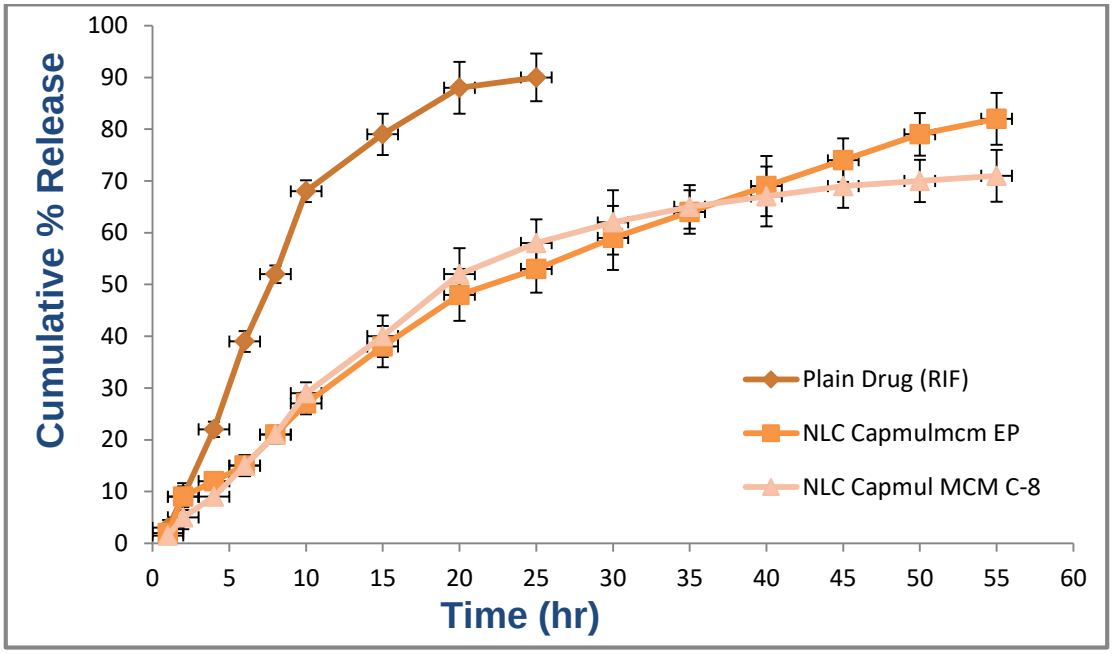

Fig: 5.30- Graphical presentation of In-vitro release Profile

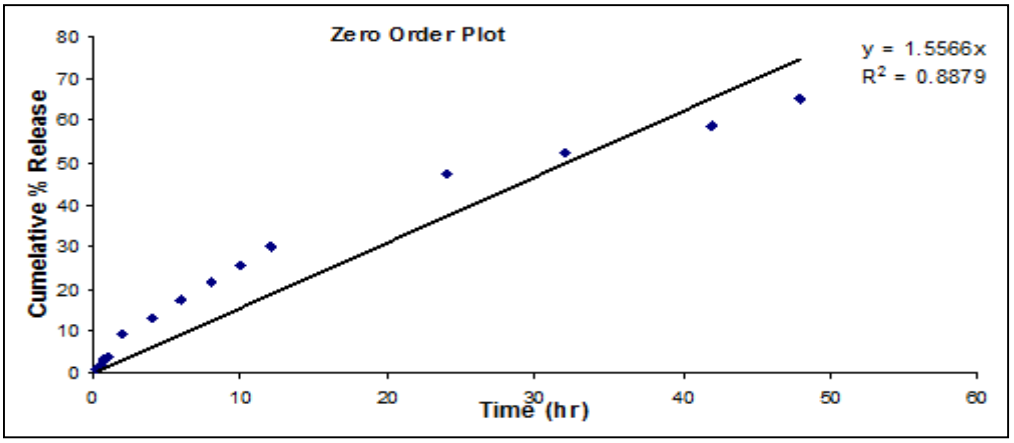

Fig: 5.31- Graphical presentation of zero order reaction

Zero Order		First Order		Higuchi		Koresmeyer- Pappas	
r^2	K_0 (h^{-1})	r^2	K_1 (h^{-1})	r^2	K_H ($h^{-1/2}$)	r^2	N
0.887	1.556	0.985	-0.009	0.972	8.926	0.9828	0.7881

Table: 5.13- Release Kinetic of Optimised batch

5.10 Cell Culture Studies

5.10.1 Establishment and maintenance of cell lines

A human macrophage cell line (J7441.A) (purchased from NCCS Pune) was grown as monolayer using RPMI supplemented with 5% fetal bovine serum. The media was supplemented with 100 µg/ml penicillin and 100 µg/ml streptomycin to depress the growth of micro-organisms. Cell lines employed in this study was maintained in a humidified incubator at 37±2ºC with 95% air and 5% CO_2. Cells were sub-cultured twice weekly by simply re-suspending the cells using 0.2 % Trypsin 0.025% EDTA and then replacing half of the cells suspension with a fresh medium. Adherent cells were grown to 80% confluence in tissue culture grade flasks and were sub cultured by discarding the used medium, leaving the cells adhered to the bottom of the flask (Hoellenriegel, et al., 2011).

5.10.2 Viable cell counts

Viable and non-viable cells were distinguished using the hemocytometer, for this purpose, trypan blue was used. Live cells can exclude the trypan blue stain, leaving them with a normal appearance under the microscope. Dead cells, however take up the stain making them appear blue. An equal volume of cells and stain (0.4%) were mixed and applied to the bright-line haemocytometer. The number of cells counted (ignoring blue cells) was multiplied by $2x10^4$ to calculate cells/ml, thus taking into account the dilution factor upon addition of the trypan blue.

5.11 Cell Cytotoxicity Studies

5.11.1 (Modified Microculture Tetrazolium Assay)

The modified microculture tetrazolium assay was used to assay the IC_{50} (drug concentration that caused 50% inhibition of cell proliferation/cytotoxicity) of Rifabutin on J 7441.A macrophage cells in both the formulation. Briefly, cells harvested from exponential phase cultures were counted by trypan blue exclusion (only cell preparations demonstrating viability >90% were used) and dispensed within 96-well flat-bottomed Costar (Cambridge, MA) culture plates (10000 cells/100 µl per well for a 3-day incubation) (Jing, et al., 2010).

Table 5.14: Cytotoxicty of NLCs in J744.1 Macrophage Cells by MTT Assay

Formulation	IC_{50} Value (µM)
Plain Drug Solution	1.34
NLC CAPMUL EP	2.58
NLC CAPMUL C-8	5.12

5.12 Spectrofluorimetric Analysis

5.12.1 Cell Uptake Studies

Calcein loaded NLCs were prepared to study their uptake to Macrophage cell line J7441.A. Plain calcein loaded NLCs with both type of formulation were prepared (Capmul MCM EP and Capmul MCM C-8) were assayed. The calcein loaded NLCs were prepared by similar method. The calcein is used in concentration 0.5mg/ml in PBS instead of drug. The calcein loaded NLCs were purified from unloaded calcein with Sephadex G-50 column.

Both type of formulations were diluted in 1 ml RPMI solution and added to monolayers of J7441.A macrophage cell lines ($2x10^5$) grown in 96 wells culture plate and incubated for 30, 60, 120, 180 and 240 min at 37ºC. Cell monolayers were thoroughly washed in phosphate buffered saline (PBS), and lysed in 0.75 ml of lysis buffer (PBS containing 0.1% Triton X-100). The fluorescence was measured in the lysis buffer extract using Shimadzu fluorescence spectrophotometer at excitation and emission wavelength of 661 nm.

Table:5.15- Cell uptake of NLC Capmul MCM EP and NLC Capmul MCM C-8 formulations (surface bound and internalized)s

Time (min)	Fluorescence Intensity	
	NLC Capmul EP	NLC Capmul C-8
30	58	368
60	73	590
120	87	752
180	96	798
240	99	814

The cell surface-bound NLCs were stripped by two washes with acidic saline (0.9% NaCl adjusted to pH 3 with acetic acid) followed by two washes with PBS to determine the fraction of internalized NLCs. The remaining fluorescence was considered as internalization. Data of

time kinetics of fluorescence related cell uptake study of internalized formulations was recorded (Stamatopoulos, et al., 2012).

5.12.2 Fluorescent Microscopy

Fluorescent Microscopy was done on both NLCs formulation. Cells were cultured in 6-well plastic dishes containing 18mm cover slips for 24 hr. Calcein loaded NLCs were added to the cell culture media RPMI, at a particle concentration of 0.10 mg/ml. After 3 h of incubation at 37ºC, the cells were washed six times with PBS. The cover slips were put on slides coated with buffered mounting medium and viewed by Olympus fluorescence microscopy (Japan) as shown in Photomicrograph (Meijering, et al., 2004).

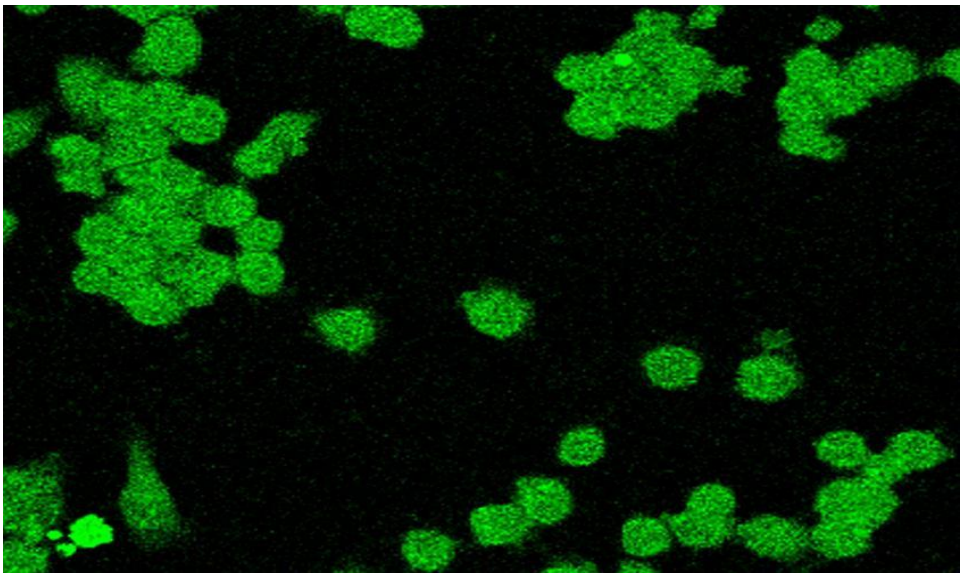

Figure:- 5.32 Florescence Image of Capmul MCM C-8 With Calcein- I

Cell uptake was measured in this part of the study. Cell uptake of J744A.1 human macrophage cells was studied. J744A.1 cell lines were incubated with calcein loaded Nano lipid carrier with drug to the cell culture media RPMI, at a particle concentration of 0.10 mg/ml. After 3 h of incubation at 37±2ºC, the cells were washed six times with PBS. To distinguish surface bound Nano lipid carrier, J744A.1 cells were washed with either cold PBS to remove unassociated Nano lipid carrier or acidic saline to strip bound but not internalized Nano lipid carrier. The cells were then lysed and assayed for residual cell fluorescence using the protocol described above. The results showed that uptake was 63.17 shown NLC Capmul mcm C-8 formulation. Intensity of fluorescence was exhibited maximum. Uptake of calcein loaded Nano lipid carrier.

The uptake of the calcein loaded Nano lipid carrier by J744A.1 cell lines were visualized using fluorescence microscopy. The intense cell-associated fluorescence in the sample containing coupled Nano lipid carrier and drug coupled with calcein revealed that calcein loaded Nano lipid carrier formulation was more taken up by the J744A.1 macrophage cell line than that of plain drug as the intensity of fluorescence was shown maximum by the calcein loaded Nano lipid carrier formulation.

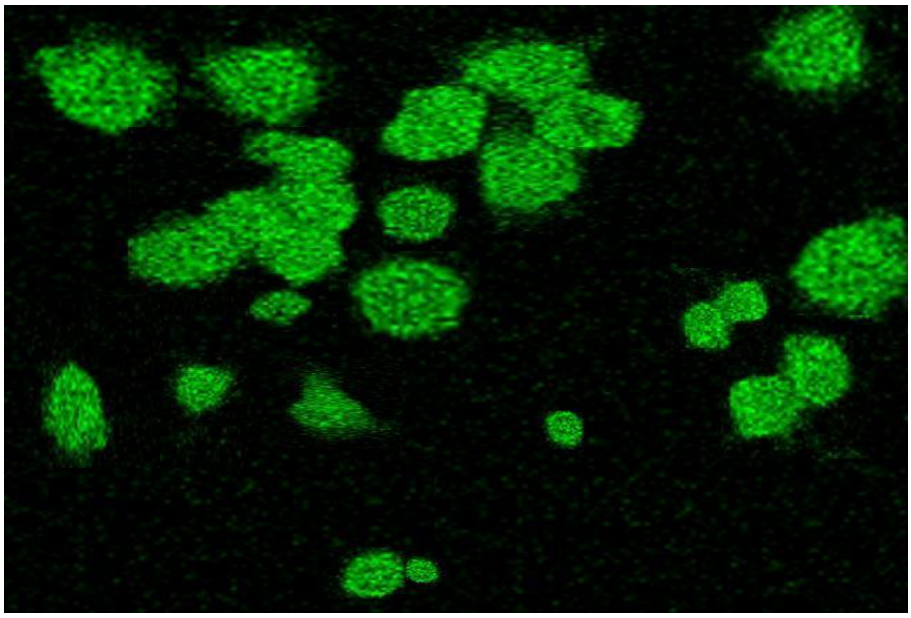

Figure:- 5.33 Florescence Image of Capmul MCM C-8 With Calcein- II

5.13 Stability Studies

Stability is of immense importance in the development of pharmaceutical formulations and plays an important role in the final design of a safe and efficacious drug delivery system. The purpose of stability testing is to provide evidence on how the quality of a formulation varies with time under the influence of a variety of environmental factors such as temperature, humidity. Degradation is likely to occur under tropical conditions of higher ambient temperature and humidity. The present study is desired to test the stability of Nano lipid carrier based formulation of Rifabutin drug.

The stability study on prepared formulation was performed by storing the formulation at low temperature that is 4±2ºC , 30±2ºC, 45±2ºC for 06 month and formulations were assessed periodically for the change in Particle size, and residual drug content.

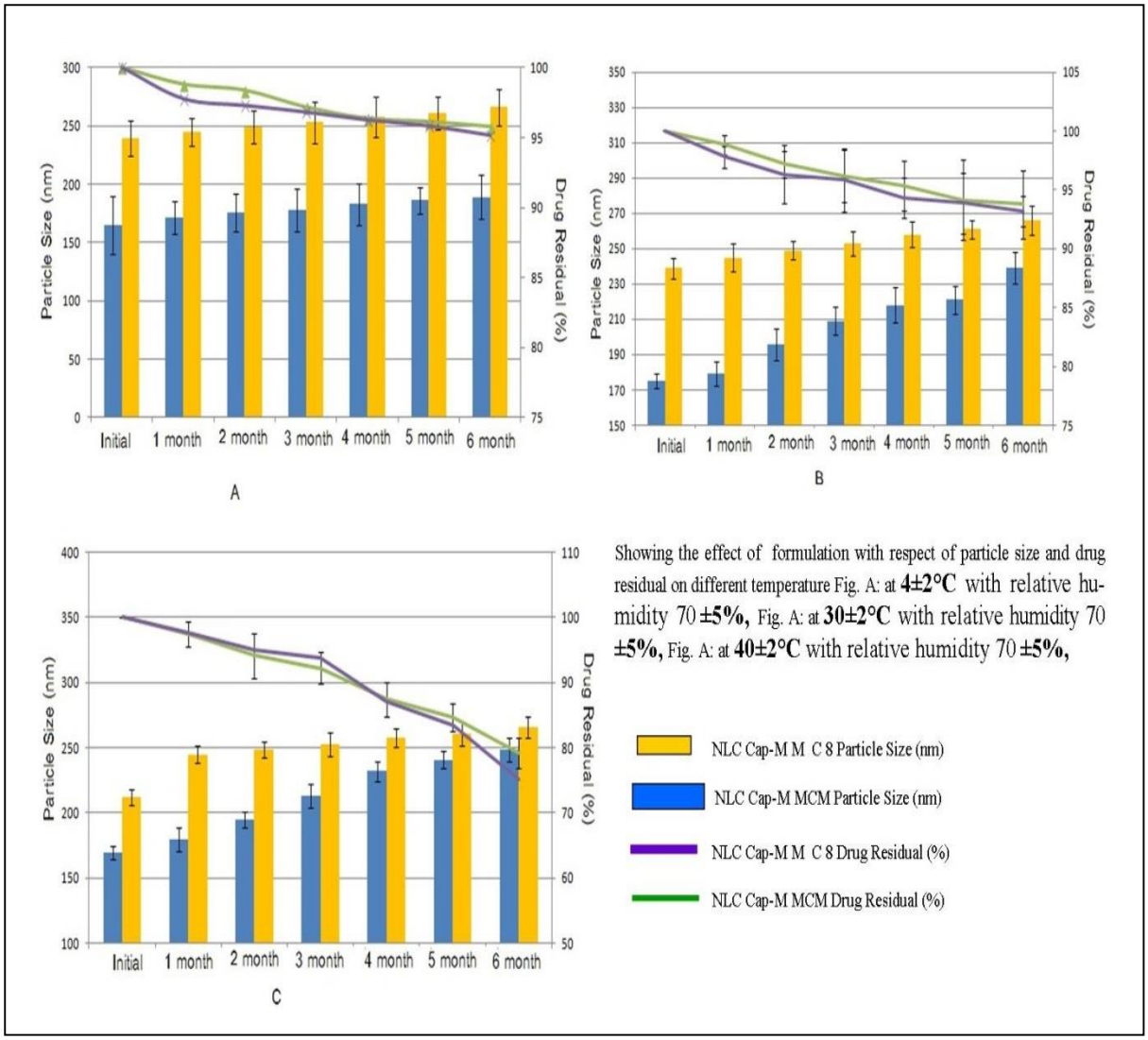

Fig: 5.34-Graphical presentation of stability studies at different temperature

5.14 Differential scanning calorimetric (DSC) study

DSC analysis was done to study the state of Rifabutin inside the NLCs. DSC thermo grams of Rifabutin are illustrated in Figure 5.30. DSC curve of pure Rifabutin showed a sharp endothermic peak at 171ºC, corresponding to the melting point of Binary mixture and presirol ATO 5 has showed his peak at different temperature which indicated the non-interaction.

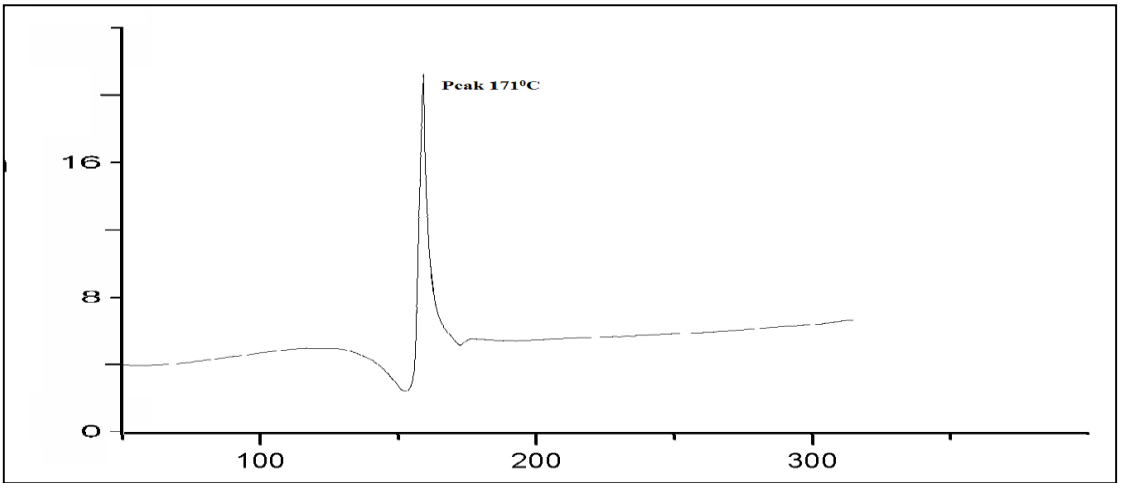

Fig: 5.35-DSC Image of Rifabutin drug

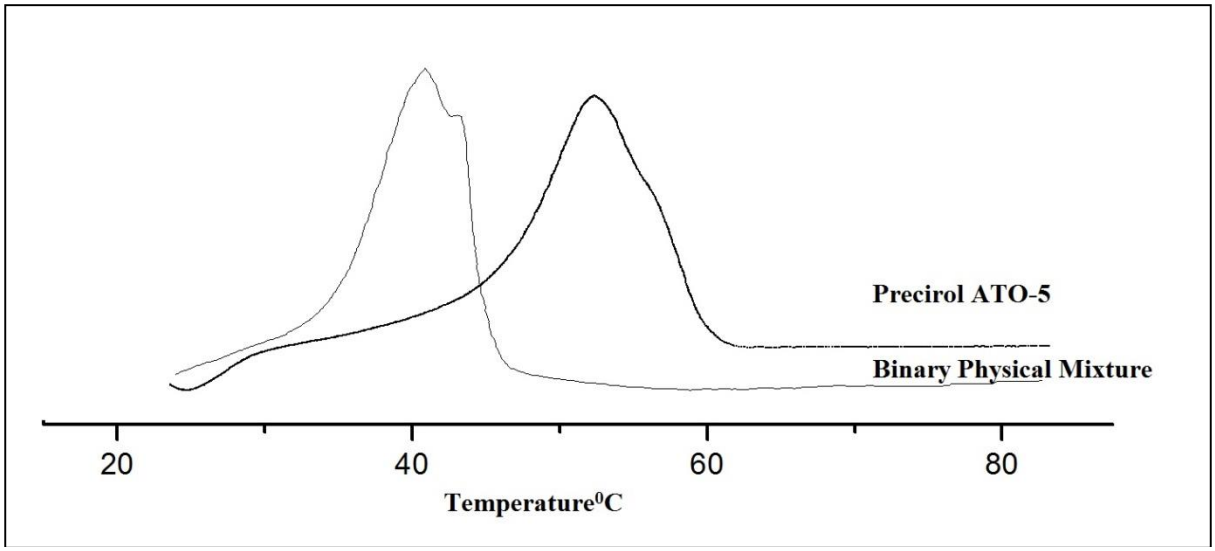

Fig: 5.36-DSC Image of Precirol ATO 5 and binary physical mixture at different Temp.

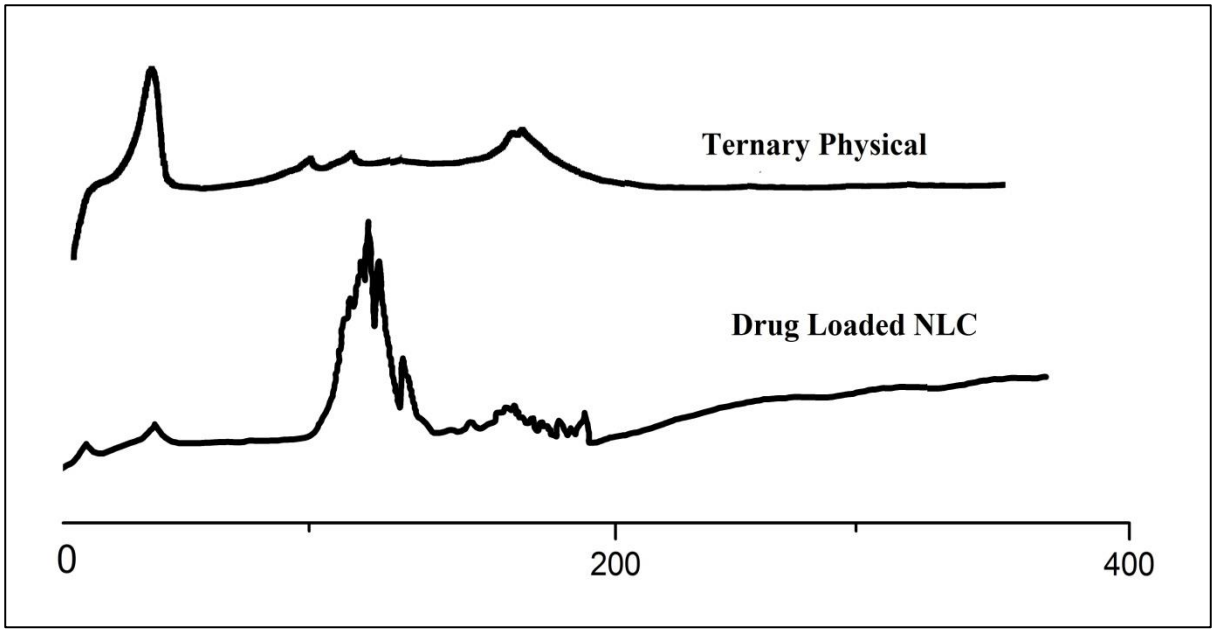

Fig: 5.37-DSC Image of Ternary Physical with Drug Loaded NLC

Whereas Drug loaded NLCs showed a broad peak at about 110°C as well as a small depressed peak at 130 to 185°C. Broad peak showed the characteristic of the drug loaded NLCs while depressed peak indicated interactions between drug and lipid which occurred during the production process, which can distort crystallization and result in a lower melting enthalpy.

5.15 Pharmacokinetic study in serum

The results of both the sets of *in vivo* studies involving 24 wistar rats in each set were merged and mean values were taken for analysis. The *in vivo* studies clearly revealed that the pharmacokinetics of rifabutin were significantly altered when delivered through NLC loaded with drug. Plasma concentration-time profile and pharmacokinetic data in Figure 5.33 and Table 5.14, respectively, clearly indicate that the free rifabutin solution rapidly cleared off from the blood circulation and was detected only till the 22^{th} h following single intravenous administration. In contrast, plasma level in the case of NLC-EP and NLC C-8 remained for a longer period, though; the plasma level of NLC-EP was lower than that of NLC-C8 at each time point. This may be due to the relatively rapid uptake of NLC-EP by macrophage-rich organs in comparison to NLC-C8. Also, the data shown in Table 5.15 clearly indicate that mannose conjugation resulted into significant improvement in the value of MRT (mean residence time) ($p<0.05$; One way ANOVA).

Table No-5.16. Different Variable of Pharmacokinetic studies

Ethical Approval	Central animal ethical committee of the university
Animal	Wistar Rat
Weight	250-300 g
Number of groups	4 (6 animals each)
Samples	Rifabutin solution/ NLC Capmul-EP/ NLC Capmul-C8
Dose	2 mg/kg
Rout of administration	Intravenous (Tail Vein)
Blood collection	Retro orbital vein (200µL; after either anesthesia)
Timing	0, 06, 12, 36, 48 and 60 hrs
Analysis	HPLC method
Calibration	10 to 5000 ng/ml
Pk Profile	Plasma concentration Vs Time
Pk Software	Kinetica 5.0
Pk Analysis	Using non-compartmental intravenous analysis

Table No- 5.17, Results of Pharmacokinetic studies

S. No	Parameters	Plain Drug	NLC Capmul MCM EP	NLC Capmul MCM-C8
1	C_{max}	62.6000	36.0000	45.0000
2	T_{max}	6.0000	24.0000	24.0000
3	AUC_{last}	530.534	1404.2762	1654.1395
4	AUC_{total}	578.810	1801.5898	2470.0834
5	$t_{1/2}$	5.576	22.9497	29.7667
6	MRT	11.5298	42.7415	55.0936

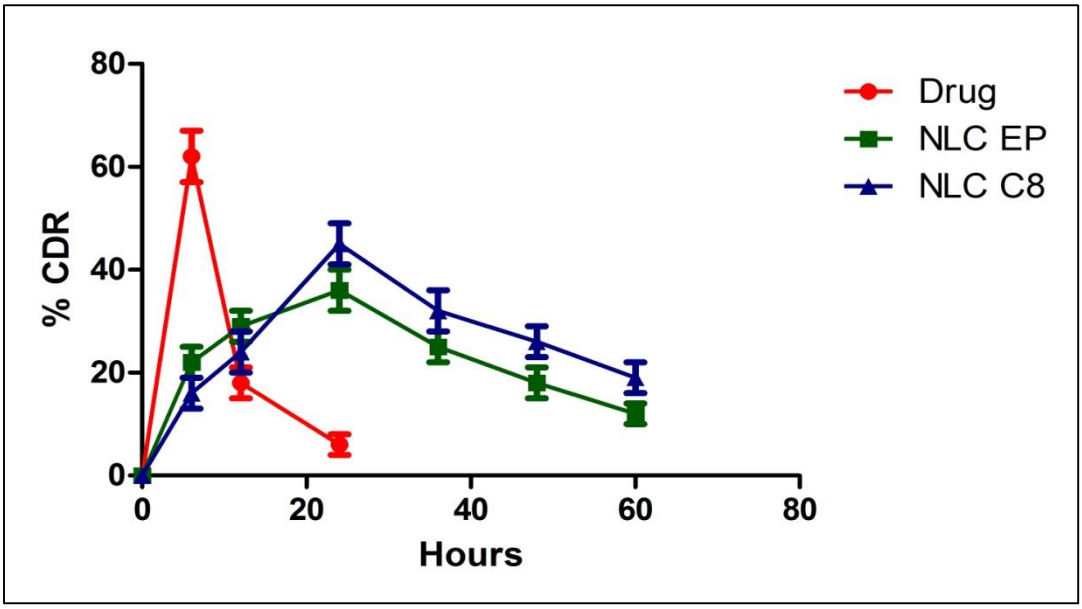

Fig. 5.38- % Cumulative Release of plain drug with other formulations